# 國 立 交 通 大 學

## 生物科技研究所
## 碩士論文

利用定點突變進行氧化鯊烯環化酵素家族

假設活性區中胺基酸之特性探討

# Investigating the Characteristics of Putative Active-Site Amino Acids in Oxidosqualene Cyclases by Site-Directed Mutagenesis

研究生：陳奕齊

指導教授：吳東昆 博士

中華民國九十九年

# Investigating the Characteristics of Putative Active-Site Amino Acids in Oxidosqualene Cyclases by Site-Directed Mutagenesis

研究生：陳奕齊　　　　　　　　　Student: Yi-Chi Chen

指導教授：吳東昆　博士　　　　　Advisor: Dr. Tung-Kung Wu

國立交通大學

生物科技研究所

碩士論文

A Thesis
Submitted to Department of Biological Science and Technology
College of Science
National Chiao Tung University
in partial Fulfillment of the Requirements
for the Degree of
Master
in
Biological Science and Technology
July, 2010
Hsinchu, Taiwan, Republic of China

中華民國九十九年七月

# 利用定點突變進行氧化鯊烯環化酵素家族

# 假設活性區中胺基酸之特性探討

學生：陳奕齊　　　　　　　　　　　指導教授：吳東昆　博士

國立交通大學　生物科技研究所　碩士班

## 摘要

氧化鯊烯環化酵素存在於大多數生物體之中，他們會將直鏈狀的氧化鯊烯，反應成特定的多環結構。在不同的生物物種，例如植物、動物與真菌間，會經由不同的反應機制而形成不同的產物。催化過程包含氧化鯊烯上環氧基開環的起始反應、中途複雜的環化和重組的步驟、以及最後的去質子反應，形成高度專一性的產物。為了比較不同類型的氧化鯊烯環化酵素，我們選用了酵母菌中的氧化鯊烯-羊毛硬脂醇環化酵素、阿拉伯芥中的環阿屯醇環化酵素及豌豆中的 β-麥胚固醇環化酵素這三種來利用定點突變的方式，分析存在於酵素活性區中的相對應胺基酸，希望能從實驗分析找出它們的功能以及重要性。

在酵母菌的氧化鯊烯-羊毛硬脂醇環化酵素實驗中，我們利用定點飽和突變的方法，針對 Cys703 來做分析。分析結果顯示經由不同的胺基酸突變，產生了八種不同的產物，除了原先就會產生的羊毛硬脂醇之外，產生六種已知的環化中間物和一個先前未曾被發現過的未知物。而其中之一的四環產物較為被關注，它在十七號碳的型態擁有向上的氫和向下的長碳側鏈，與正常的結構相反，所以可以得知 Cys703 在決定十七號碳上的側鏈為向上或向下型態佔有一定的重要性。此外，除了此產物以外，其他環化中間物皆和 Phe699 突變點的分析十分類似，加上與離受質較遠的 Cys703 相比，

Phe699 為活性區第一層胺基酸且影響力大，可以推測 Cys703 和第一層胺基酸的穩定性息息相關。

另一方面為阿拉伯芥中的環阿屯醇環化酵素及豌豆中的 β-麥胚固醇環化酵素的分析。前者與氧化鯊烯-羊毛硬脂醇環化酵素相同，在受質的摺疊會經由椅形-船形-椅形形成原脂醇碳陽離子中間物；而後者則會經由椅形-椅形-椅形形成達瑪烯碳陽離子中間物。此兩種酵素經由不同的結構和機制，分別形成環阿屯醇及 β-麥胚固醇。實驗分析方法是利用丙胺酸掃描法，選定十五個不同位置的胺基酸做突變，探討產物的差異性。在環阿屯醇環化酵素的定點突變中，產生了一些和氧化鯊烯-羊毛硬脂醇環化酵素突變中出現過的產物，推測是因為結構和機制非常的類似，因此儘管是不同物種，但還是可以經由突變而產生相同的產物。而在 β-麥胚固醇環化酵素的定點突變中，只分析出兩種產物，推測可能是因為在 β-麥胚固醇環化酵素這種椅形-椅形-椅形的機制中需要比較精確的結構才可以使反應穩定，而詳細的反應機制則需要更進一步地針對活性區周圍的胺基酸做深入的研究。

# Investigating the Characteristics of Putative Active-Site Amino Acids in Oxidosqualene Cyclases by Site-Directed Mutagenesis
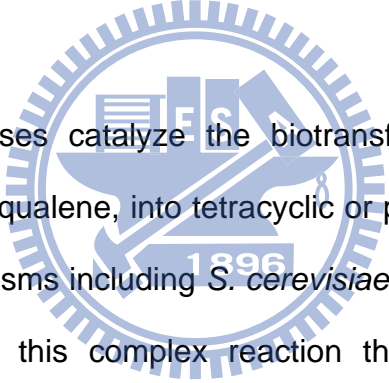
Student: Yi-Chi Chen                    Advisor: Dr. Tung-Kung Wu

Institute of Biological Science and Technology

National Chiao Tung University

## Abstract

Oxidosqualene cyclases catalyze the biotransformation of the linear form substrate, (3$S$)-2,3-oxidosqualene, into tetracyclic or pentacyclic triterpene product. Different species of organisms including *S. cerevisiae* ERG7, *A. thaliana* CAS1 and *P. sativum* PSY operate this complex reaction through different conformation intermediates within the oxidosqualene cyclization process. According to previous reports, by utilizing the diverse structural and stereochemical control in various catalytically important amino acid residue mutants, oxidosqualene cyclases produced diverse product profiles ranging from monocyclic to polycyclic triterpene alcohols. These data implied that the plastic enzyme could thus be redesigned to obtain a novel reactivity from this complex enzyme, but with the characteristics of well-known high product specificity. Moreover, in order to further illustrate other critical amino acids involved in the catalytic significance and enzymatic plasticity of ERG7, CAS1 and PSY, we described herein a series of site-saturated mutations on

the Cys703 residue of ERG7 and fifteen alanine-scanning mutations of CAS1 and PSY, respectively.

In the mutations of Cys703, a diverse products profile, including four known truncated cyclization tricyclic structures, four known tetracyclic structures and a novel product were identified from various ERG7$^{C703X}$ mutants. The product characterization and homology modeling results suggested that the Cys703 may indirectly affect the C-17 cation stabilization and the final deprotonation step, via the intermediary of the Phe699 residue, resulting in the production of either 17α or 17β side chain product derivatives. Structure-function-mechanism relationships of Cys703 and Phe699 on the catalytic activity of OSC could thus be discussed in a series of ERG7$^{Phe699X/Cys703I}$ double mutants.

In parallel, alanine-scanning mutagenesis was carried out on putative active site residues of CAS1 and PSY to further analyze the mutagenic effect on oxidosqualene cyclization in different sources. For mutation on CAS1, the product profiles of different mutants showed that there are highly relevant comparisons between CAS1 and ERG7. For example, the same bicyclic compound (9$R$,10$S$)-polypoda-8(26),13E,17E,21-tetraen-3β-ol was found in the CAS1$^{Tyr734}$ mutant and its corresponding residue in the ERG7$^{Tyr707}$ mutant. The results show that although they exist in totally different species, the relationships between them are still relevent. For the PSY mutation, there were only β-amyrin and lupeol synthesized from these mutants. This phenomenon allows us to predict that the producing of β-amyrin in PSY needs more precise structural control of substrate in the enzymatic active site. Thus, the detailed understanding of critical residues should be investigated after the functional roles of the neighboring amino acids in the active site are confirmed.

# 謝誌(Acknowledgement)

究，在平常生活上除了是需要幫忙時的好救兵外，也是聊聊天調濟心情的好對象。而即將變成小老大的學弟妹們，首先感謝你們在準備我們口試時花了不少心力。而對於OSC 組的怡臻和欣怡，妳們總是為了我們組不辭辛苦的幫忙，感謝妳們默默地接受這些不人道的虐待，是我能順利完成實驗的幕後功臣，OSC 組以後還要麻煩妳們了。世穎身為唯一的碩班學弟，感謝你總是幫忙我處理些實驗室的工務雜務，日常生活上也受到了很多的幫助。欣芳除了總是很溫柔地笑臉迎人、帶給實驗室不錯的氣氛外，也是聊天的好對象。而在專題生小朋友方面，球球是我最感謝的人，最重要的是我實驗上純化未知物的救星，而且在其他小事方面總是不辭辛勞地當我的小幫手。小彥除了一手包辦了實驗室的歡笑，帶給實驗室很多的活力外，在生活上也幫了我不少忙。奕汝和瑛婷對於實驗室的雜務幫忙了不少，另外妳們的實驗態度也是我一直在學習的地方。而對於最近新進的碩一學弟妹和專題生，有你們的加入，讓實驗室充滿了新鮮和活力的氣息，讓我做實驗的精神又為之一振。

當然也要感謝我的家人，總是提供我一個無後顧之憂的環境，並且在我的目標和方向總是持續地支持，在我遇到困難時絕對會全力幫忙，另外在求學和實驗方面總是給我很多的建議。

陳之藩的《謝天》一文結尾說到：「要感謝的人太多了，不如就感謝天吧！」我想，這應該就是我現在心裡的最佳寫照吧！最後在這裡，再次衷心地感謝這兩年來在我身邊的每一個人，並祝你們也天天精彩、豐富。

# Table of Contents

# List of tables

# List of Figures

# Chapter 1   Introduction

## 1.1   The importance of sterols

Sterols play important roles in living cells. They usually process a tetracyclic or pentacyclic ring structure, and they are the product of the cyclization of triterpenoids. Moreover, they are known as steroid alcohols with a hydroxyl group at the C-3 position of the A-ring.

Cholesterol is the most important sterol in vertebrates. It is a primary component of the cell membranes and serves as an intermediate in the biosynthesis of most of the important steroids. Therefore, it is essential to life. Cholesterol circulates in the bloodstream and is synthesized by the liver and several other organs. However, high levels of blood cholesterol have been implicated in the development of arteriosclerosis and in heart attacks that occur when cholesterol-containing plaques block arteries supplying the heart, so some treatments to reduce blood cholesterol are usually required.

Steroid derivatives have various functions as well. For example, many higher plants contain steroid saponins and sapogenins. Diosgenin, one of the steroid sapogenins, is the starting material of industrial interest in the synthesis of several steroids that are used as anti-inflammatory, androgenic, estrogenic, and contraceptive drugs on the market. Furthermore, these compounds are reported to possess cytotoxic, antitumor, antifungal, immunoregulatory, hypoglycemic, and cardiovascular properties.[1]

## 1.2   Terpenes, sterols and their biosynthetic pathway

Terpenes are derived biosynthetically from units of isoprene, which has the

molecular formula $C_5H_8$. The basic molecular formula of terpenes are multiples of the isoprene unit $(C_5H_8)_n$, where n is the number of linked isoprene units. Triterpenes are derived from six isoprene units, and have a formula $C_{30}H_{48}$. In some biosynthetic pathways, they are converted into triterpenoids, a family of oxygen-containing compounds. For example, the acyclic triterpene, squalene, is an important metabolic precursor of sterols.

The sterols biosynthesis process is generally through the mevalonic acid (MVA) pathway. Acetyl-CoA ($C_2$) is condensed into acetoacetyl-CoA ($C_4$) with another acetyl-CoA subunit via the acetyl-CoA transferase triggered reaction. By 3-hydroxy-3-methylglutaryl-CoA (HMG-CoA) synthase, acetyl-CoA condenses with acetoacetyl-CoA into HMG-CoA ($C_6$). HMG-CoA is converted into mevalonate ($C_6$), after the catalysis of HMG-CoA reductase. Mevalonate is phosphorylated by three sequential Pi transferred from ATP, yielding 3-phospho-5-pyrophosphate ($C_6$). Moreover, by undergoing decarboxylation, coupled with dehydration, isoprenoid pyrophosphate ($C_5$) is generated. Isopentenyl pyrophosphate is referred to isoprenoid in the pathway. By a series of chemical reactions, including isomerization and condensation, a linear molecule, squalene ($C_{30}$), is produced.

In bacteria, squalene is made via different compounds via various enzymatic reactions. Squalene is largely converted to hopene by squalene-hopene synthase, and can be catalyzed into hopanol or diplopterol via other enzymes. However, in most eukaryotes, the oxidation of squalene by squalene synthase yields an acyclic polyolefin substrate, (3*S*)-2,3-oxidosqualene (OS), which is the precursor of steroids.

In higher plants, the cyclization of OS can be transformed into cycloartenol, lupeol, and β-amyrin by cycloartenol synthase, lupeol synthase, and β-amyrin synthase, respectively. Furthermore, the OS can also convert into lanosterol by

oxidosqualene-lanosterol cyclase, in fungi and animals. After a series of cyclization and/or rearrangement cascades, depending on the forming species, the steroids are formed with diverse structures **(Fig. 1.1)**.
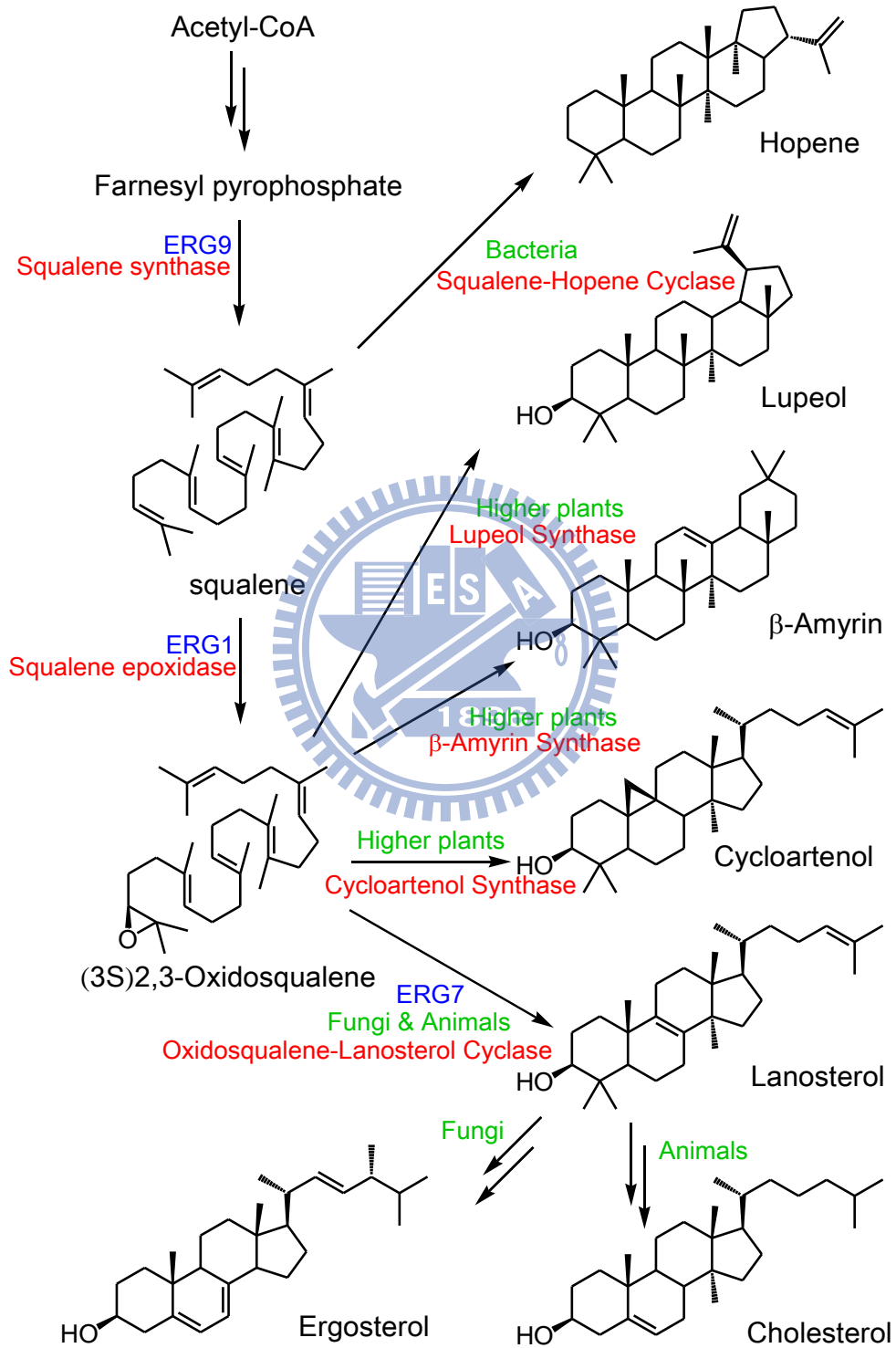


**Figure 1.1 The sterol biosynthetic pathway.**

## 1.3    Triterpene cyclases family

The triterpenoids are a large and structurally diverse group of natural products derived from squalene or other acyclic 30-carbon precursors.[2] The unusually complex reaction mechanism and flexible reactant structure generates these ring systems and results in over 100 distinct steroid skeletons. Enzymes that catalyze these reactions are known as triterpene synthases and can be categorized as squalene cyclases or oxidosqualene cyclases, which convert squalene and oxidosqualene to diverse sterols. The enzymatic cyclization of squalene or oxidosqualene to polycyclic triterpenoids is one of the most complicated biochemical reactions to capture the interest of organic chemists and biochemists for over half a century.

There is a general mechanism among these enzymes, involving:

1.  Binding of the polyolefinic substrate in a folded conformation.
2.  Initiation of the reaction by protonation of a double bond (in squalene scaffold) or an epoxide (as shown in OS scaffold).
3.  Ring formation.
4.  Skeletal rearrangement by methyl and hydride shifts in some cases.
5.  Termination by deprotonation or addition of water.[3]

However, there are still many differences in their mechanisms. The enormous skeletal diversity found among the triterpenes is the result of different cyclization reactions that lead to varied carbocyclic skeletons, following by different methyl and hydride shifts and a different cation-quenching step.

The substrate in these enzymes is pre-folded into different conformations. In squalene-hopene cyclase SHC, the binding substrate squalene is only pre-folded into the all-chair conformation. However, there are two folding types within oxidosqualene cyclases, chair-chair-chair and chair-boat-chair conformations,

respectively.

1. Chair-chair-chair conformation:

   This conformation has been found in higher plants, including lupeol synthase and β-amyrin synthase. The B-ring was pre-folded in chair form. When cyclization occurs, OS is converted into dammarenyl cation first. After the entire reaction, it generates the product, lupeol or β-amyrin **(Fig. 1.2 A)**.

2. Chair-boat-chair conformation:

   It is another kind of substrate folding manner when the B-ring is pre-folded in the boat form in the enzymatic active site during the cyclization process. The tetracyclic transition state compound is called the protosteryl cation. In different enzymes from various species, there are different products. Cycloartenol was generated by cycloartenol synthase in higher plants; lanosterol was produced by oxidosqualene-lanosterol cyclase in fungi and animals, respectively **(Fig. 1.2 B)**.
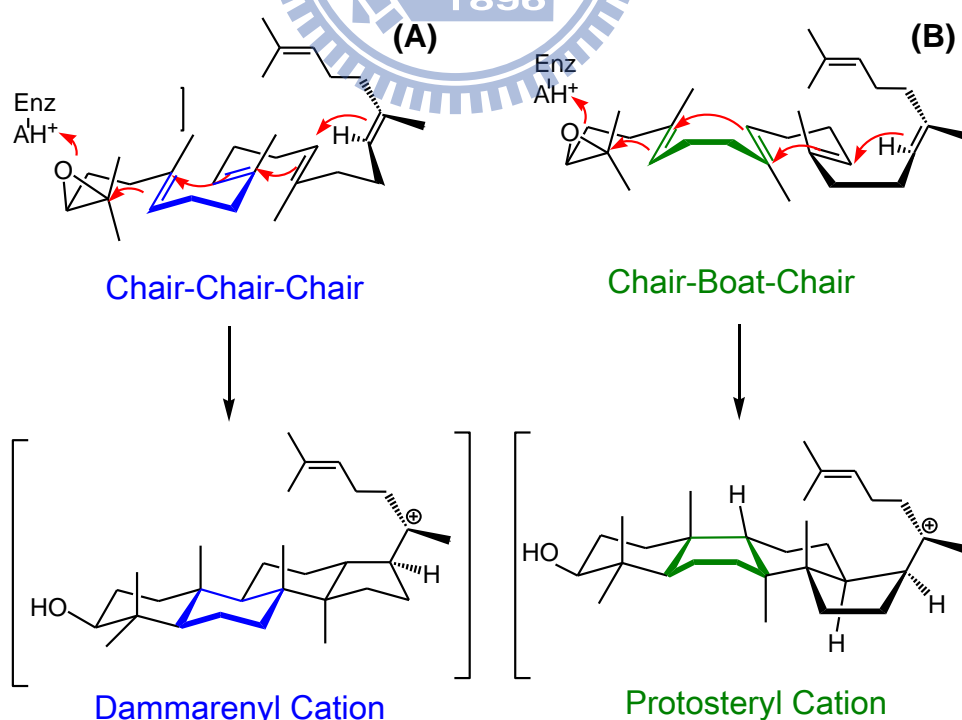


**Figure 1.2 Cyclization of (A) dammarenyl cation, (B) protosteryl cation.**

## 1.3.1 The hypothesis of oxidosqualene cyclase

The family of oxidosqualene cyclases extensively exists in organisms. These different enzyme systems convert the oxidosqualene, as a substrate, into various polycyclic triterpenes. The relationship between the enzyme structure and cyclization mechanism is extremely interesting and diverse.

Woodward and Bloch first proposed in 1953 that in the cholesterol biosynthesis pathway, lanosterol was produced after the cyclization of squalene, followed by rearrangement.[4] In 1958 and 1965, Maudgal and Cornforth groups provided evidence for 1.2-methyl and hydride shifts during lanosterol formation by incorporation experiments.[5-6] Corey and van Tamelen showed that 2,3-oxidosqualene is more efficiently incorporated in sterol synthesis than squalene, the demonstrated intermediacy of 2,3-oxidosqualene in lanosterol biosynthesis.[7-8] In addition, van Tamelen also showed that the nonenzymatic cyclization of 2,3-oxidosqualene resulted in truncated cyclization to produce a tricyclic product, suggesting that direct enzymatic control is necessary for the prevention of the chemical tendency in the formation of the five-membered C-ring, and for emergence of the biologically required six-membered C-ring.[9] In 1975, Barton confirmed that eukaryotic oxidosqualene cyclases accepted only (3S)-, but not (3R)-, enantiomers of 2,3-oxidosqualene as a substrate in the formation of lanosterol, demonstrating the highly substrate-specific property of oxidosqualene cyclases compared to squalene cyclases.[10] Guy Ourisson and his co-workers proposed the possible molecular evolution from the primitive squalene cyclases to oxidosqualene cyclases in higher organisms.[11] Furthermore, Corey and Matsuda showed that oxirane cleavage and cyclization of the A-ring are concerted and essential for electrophilic activation of the oxirane function.[12-13]

In previous research, oxidosqualene was stable in the neutral condition at room temperature for the whole day. A stronger acid such as trichloroacetic acid is

required for epoxide ring activation to promote the cyclization step.[14] Then, many unstable cation intermediates were thus formed in the cyclization process. Two hypotheses that showed how the enzyme worked to stabilize the high-energy cation intermediates were proposed. In 1987, Johnson proposed the "cation-stabilizing auxiliary" model which supposed that the Lewis acid residues on the active site provide a proton for initiation of the epoxide group, and a number of anionic sites in the cyclase enzyme which further led to the cation generation and the formation of the proper ring system. These axial negative charge residues would face toward the transition states or the intermediates for the cation stabilization, and also facilitate the ring formation of B-boat/chair ring. Therefore the B-boat ring could be promoted by the delivery of a point charge to the α-face at pro-C-8, and lowering the activation energy of the boat form rather than that of chair skeleton **(Fig. 1.3)**.[15-16] In addition, Griffin and co-workers proposed the "aromatic hypothesis" model from which the electron-rich aromatic side chain, such as Trp and Tyr, might stabilize the positively charged transition states or high-energy intermediates during the process of cyclization and rearrangement steps **(Fig. 1.4)**.[17] In this hypothesis, the aromatic residues play the role of the anions group, just like that proposed in the "Johnson model". These cation-π interactions are common features in enzyme-substrate complexes.

**Dammarenyl Cation**   **Protosteryl Cation**

⇧ denotes site for delivery of negative point charge
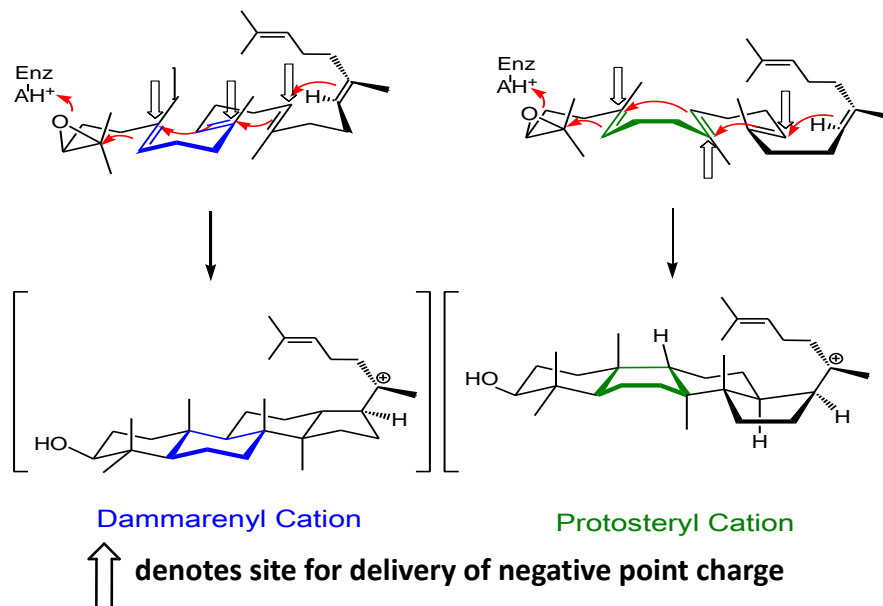
**Figure 1.3 The proposed enzyme models by Johnson**
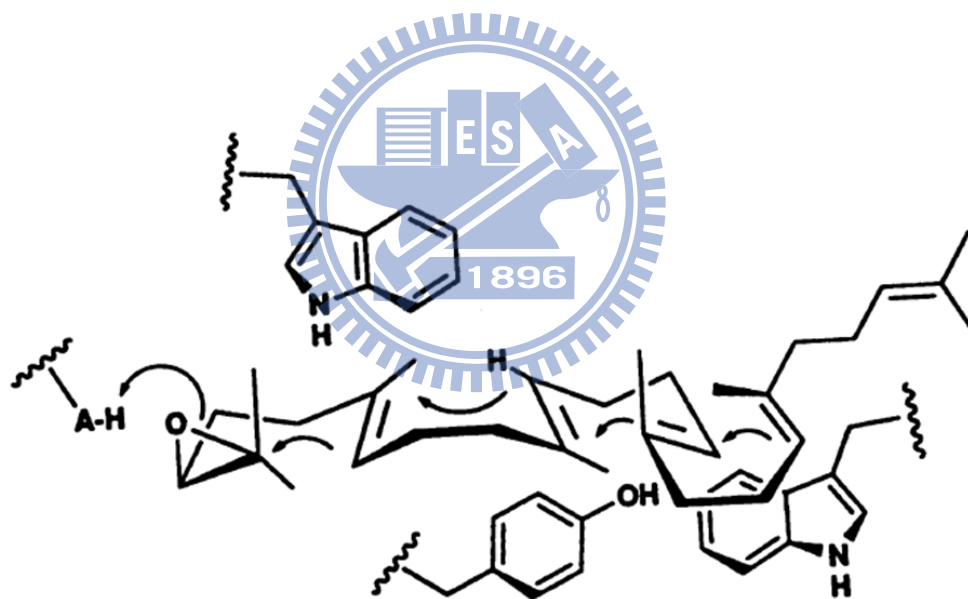


**Figure 1.4 Griffin's hypothesis model for involvement of electron-rich aromatic side chains from Trp and Tyr residues in the cyclization of oxidosqualene to the protosteryl cation.**

## 1.3.2　Squalene-hopene cyclase (SHC)

Squalene-hopene cyclase (EC 5.4.99.17) is a homodimeric enzyme which is organized in two groups of α-helical domains, which together form a dumbbell-shaped molecule **(Figure 1.5)**. It contains 631 amino acids per subunit, and the molecular masses are about 71.5 kDa each.
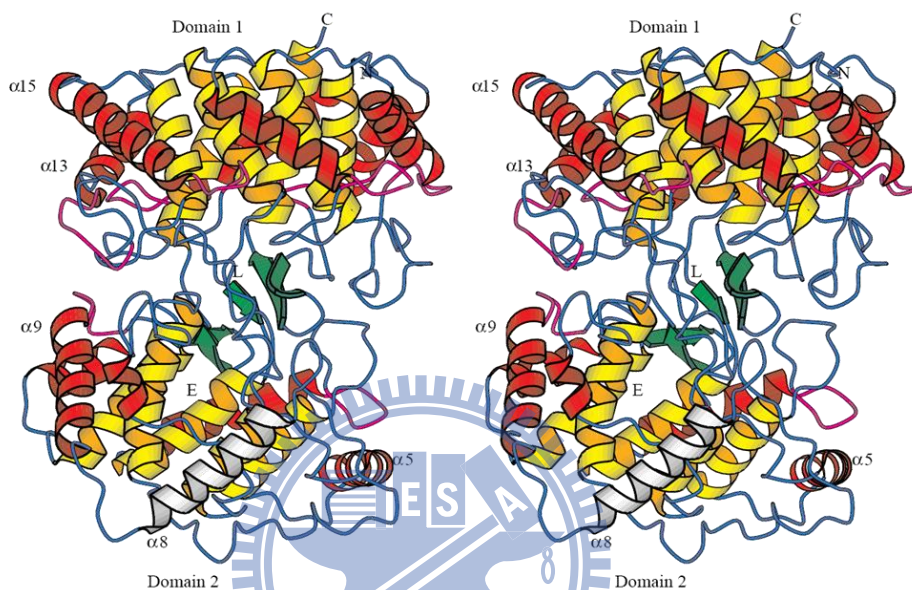


**Figure 1.5 Crystal structure of *A. acidocaldarius* squalene-hopene cyclase.**

In 1997, the X-ray crystal structure of *Alicyclobacillus acidocaldarius* SHC was first reported at a 2.9 Å resolution, later refined to 2.0 Å resolution, in 1999.[18-19] Moreover, Reinert *et al*. reported another X-ray crystal structure from which the squalene-hopene cyclase was cocrystalized with 2-azasqualene and its resolution is 2.13 Å in 2004.[20] These structures combined with the biological studies, provided a more mechanistic insight into squalene-hopene cyclases and oxidosqualene cyclases.

Squalene-hopene cyclase converts squalene to the pentacyclic hopene skeleton in prokaryotes. It binds squalene in the all-chair conformation, and initiates the cyclization cascade by protonating the terminal double bond. The cyclization reaction produces the 6.6.6.6.5-fused pentacyclic hopanyl C-22 cation, which

undergoes either proton elimination or addition of water to produce a 5:1 mixture of hopene and hopanol without the rearrangement step **(Figure 1.6)**.[21] However, the bacterial SHCs displayed very low substrate specificity. They can cyclize not only the natural substrate, but both enantiomers of oxidosqualene and regular polyprenols.
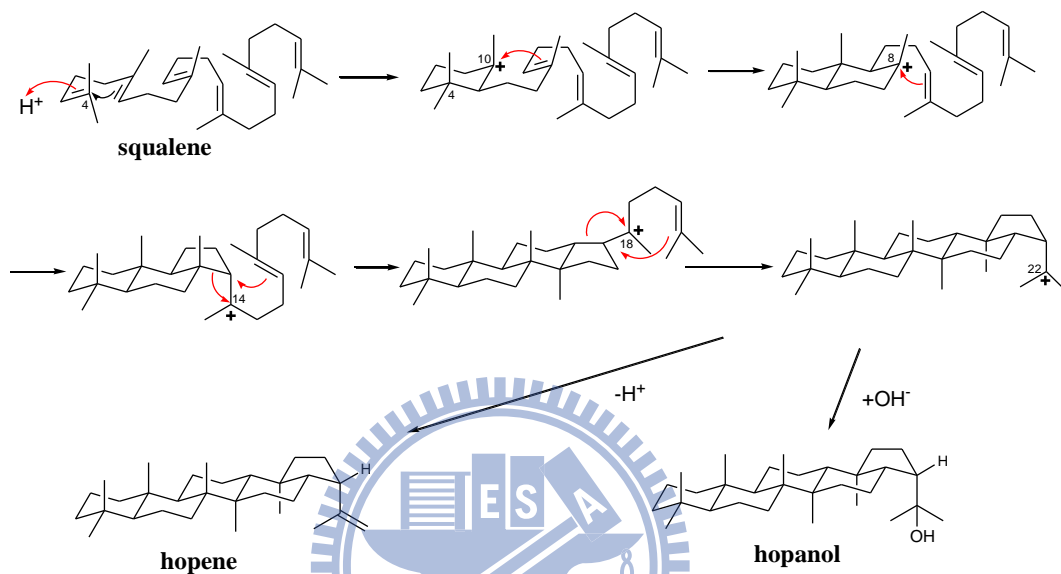


**Figure 1.6 The cyclization process of squalene-hopene cyclase.**

## 1.3.3 Oxidosqualene-lanosterol cyclase (OSC)

Oxidosqualene-lanosterol cyclase (EC 5.4.99.7), also called lanosterol synthase, is widely found in animals and fungi. It converts oxidosqualene into the tetracyclic product, lanosterol. Lanosterol is the precursor of ergosterol in fungi and cholesterol in animals, both them are important components of the cell membrane.

In *Saccharomyces cerevisiae*, cyclases are encoded from *erg7*, as a membrane protein. The protein contains 731 amino acids and the molecular mass is approximately 83 kDa. Because of the difficulty in purifying membrane proteins, the crystal structure of *S. c* oxidosqualene-lanosterol cyclases (*Sce*ERG7) enzyme has not been possible until recently. In order to understand the structure-function relationships of oxidosqualene cyclase-catalyzed reactions in depth, site directed /

saturated mutagenesis, coupled with genetic selection and products analysis, for illustrating the functional importance of these mutated residues, participating in the carbon cationic intermediates stabilization of the reaction cascade were carried out.

The mechanism of oxidosqualene- lanosterol cyclase includes substrate pre-folding, an epoxide ring opening, four rings cyclization, hydride and methyl groups migration, and a final deprotonative termination **(Fig. 1.7)**. In the detailed aspect, the enzyme catalyzed conversion of (3*S*)-2,3-oxidosqualene into a pre-folded chair-boat-chair conformation. Then, a residue Asp456 (*Sce*ERG7) provided a proton to start the reaction, permitting the formation of A-ring. In addition, some researches showed that His146 assists in the formation of hydrogen bond with Asp456, and it enhances the acidity of Asp456, to induce the epoxide ring opening **(Fig.1.8)**.[22]
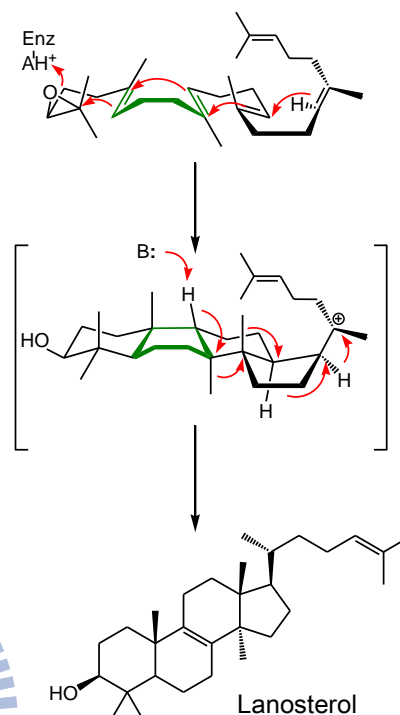


**Figure 1.7 The mechanism of conversion of oxidosqualene into lanosterol.**
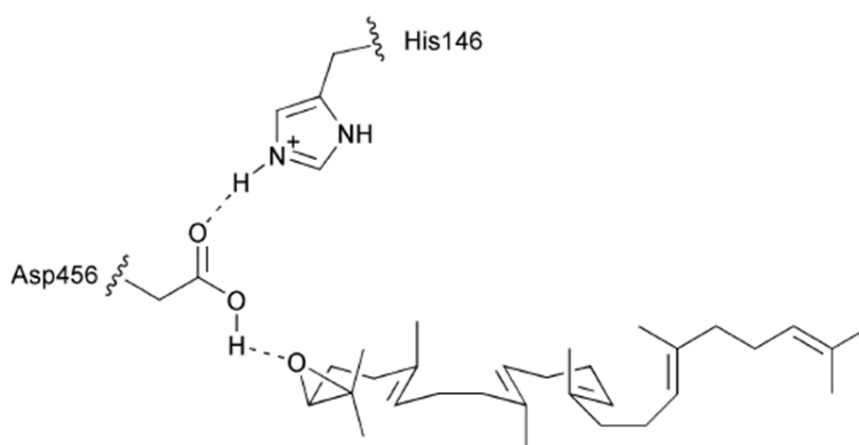


**Figure 1.8 The proposed model for oxirane ring opening and cyclization initiation.**

The formation of the B-boat ring probably occurs very rapidly when the positive charge appears on the C-6 of the A-ring. The closure of the C-ring is puzzling because the direct formation of the six-membered C-ring would represent the anti-Markovnikov form. In 1995, E. J. Corey and his co-workers first proposed the five-membered C-ring Markovnikov cyclization against the direct formation of a six-membered C-ring. By using oxidosqualene analogues, 20-oxaoxidosqualene was reacted with oxidosqualene cyclase, and the resulting products suggested that there was a five-membered C-ring intermediate appearing through an intramolecular reaction **(Fig. 1.9)**.[23] Moreover, incubation of additional substrate analogues within oxidosqualene cyclases produced 6-6-5 cyclization products, providing more evidence for a five-membered C-ring closure followed by a ring expansion.[24] In the theoretical calculation, Hess indicated that the 6-6-5-tricyclic cation was the first intermediate during the formation of the protosteryl cation, and five-membered C-ring expansion and formation of the D-ring were concerted **(Fig. 1.10)**.[25] In comparison, for the SHC study, Gao showed no and fewer intermediates of tricyclic and tetracyclic cations, suggesting that the formation of C, D and E-ring were concerted.[26]



**Figure 1.9 Substrate analogue and their product derivatives during the oxidosqualene cyclase cyclization which are suggestive of five-membered C-ring intermediates.**

12

**Figure 1.10 Proposed mechanisms for C-ring expansion and D-ring formation.**

Early studies of the sterol biosynthesis assumed that the conversion of oxidosqualene into lanosterol proceed via a protosteryl cation where its cationic sidechain at C-17 is α-oriented.[27] After a hydride migration of this 17α-protosteryl cation from C-17 to C-20, an un-natured 20*S* configuration, but not the natural 20*R* skeleton product, was thus generated. Another exception for the mechanistic illustration was suggested to explaining the backbone rotation at C20, where a 120° rotation of C17-C20 bond occurs via the hydride migration in order to produce the 20*R* skeleton of lanosterol, whereas only 60° rotation is required to produce the unnatural 20*S* configuration **(Fig. 1.11)**.[28] In recent years, it had been proposed that the 17α-protosteryl cation may not be the intermediate. In 1992, Corey proposed the evidence that stereochemistry at C-17 of the protosteryl cation prefers a β- rather than an α- orientation by the enzyme-catalyzed cyclization of 20-oxaoxidosqualene **(Fig. 1.12)**. This result overthrows the assumption that the large rotation around C17-C20 bond occurs prior to the actual rearrangement.[24,28] Moreover, the 17β-protosteryl cation was also demonstrated by the catalysis of

20,21-dehydrooxidosqualene.[29]



17α-orientation

120° rotation of C17-C20 bond

20*R*-product
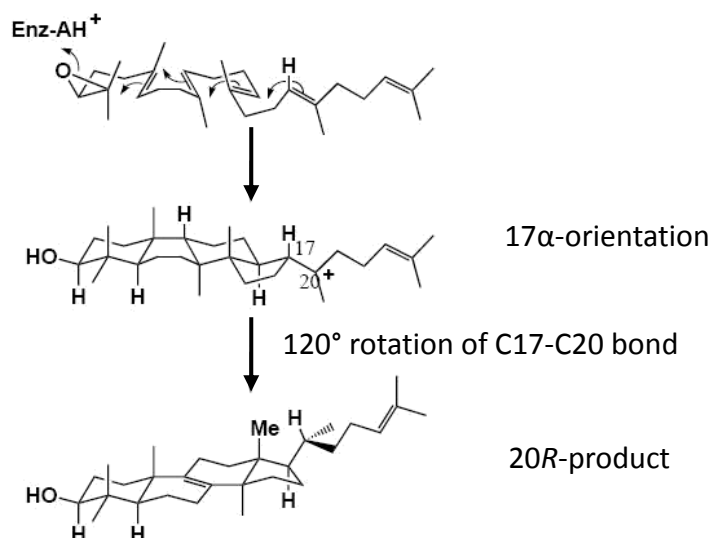
**Figure 1.11 The previous study proposed an incorrect C17α stereochemistry of protosteryl cation whereby the intermediate required a large side-chain rotation prior to rearrangement to account for the observed stereochemistry at C20.**
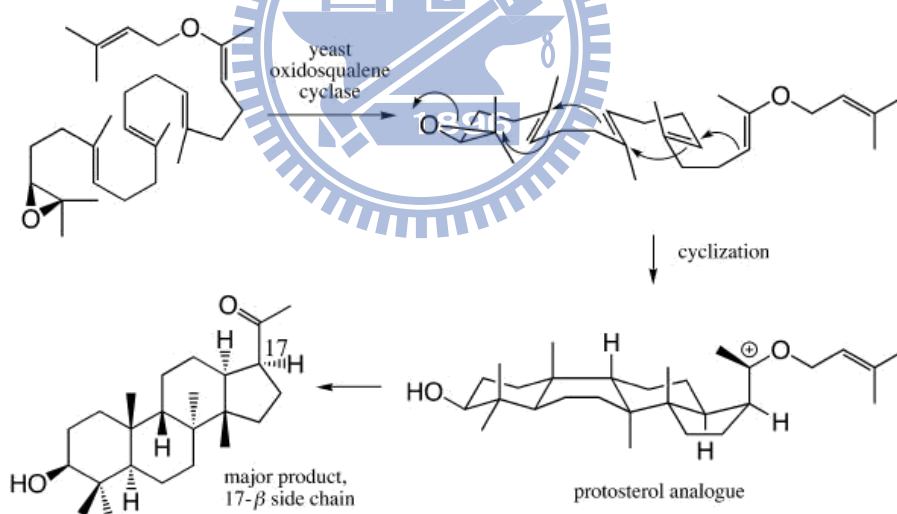


**Figure 1.12 The evidence for the stereochemistry of protosteryl cation intermediate at C17 preferring a β- rather than an α- orientation at C-17 position by incubation of substrate analogue with OSC.**

The final step of lanosterol synthesis is the rearrangement of the protosteryl cation. After two hydride and two methyl groups shift (H-17α→20, H-13α→17α, CH$_3$-14β→13β, CH$_3$-8α→14α), this is followed by deprotonation on C-8 / C-9 to

generate the product lanosterol.

In 2004, Thoma and co-workers solved the X-ray structure of human OSC which is in complex with lanosterol.[30] Human OSC is a monomer that consists of two barrel domains that are connected by loops and three smaller β-structures, and the large active-site cavity is located in the center of the molecule between domains 1 and 2. It is a monotopic membrane protein that attached to the membrane from one side, and the membrane-inserted surface consists of a plateau with 25 Å in diameter and a channel that leads to the active-site cavity. The channel is considered to permit oxidosqualene, as a substrate, to enter the hydrophobic active site and have the separated role from that of the putative active-site cavity. Achievement of the substrate passage is constructed either by a change in the side chain of the residue such as Tyr237, Cys233 and Ile524 or by rearrangement of the strained loops from 516 to 524 and from 697 to 699 **(Fig. 1.13)**. Because of the human OSC crystal structure, the relationship between the functional residues and cyclization mechanism could be understood in depth.
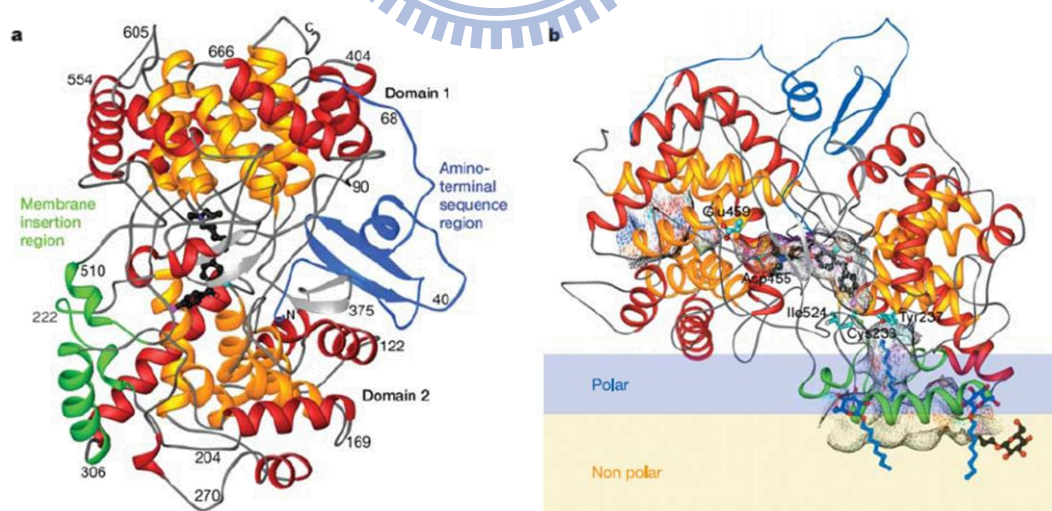


**Figure 1.13 Human OSC structure. (a) The ribbon diagram of human OSC structure. The C and N termini and several sequence positions are labeled. The inner barrel helices are colored yellow. The bound inhibitor, Ro48-8071 (black), indicates the location of the active site. (b) The orientation of OSC is shown relative to one leaflet of the membrane, and Ro48-8071 binds in the central active-site cavity.**

## 1.3.4 Cycloartenol synthase (CAS)

Cycloartenol synthase (EC 5.4.99.8) is the sterol precursor in higher plants and its skeleton is similar to lanosterol. The reaction of converting oxidosqualene into cycloartenol is very similar to that catalyzed by lanosterol synthase. Moreover, cycloartenol synthase has 759 amino acids and the molecular mass is approximately 86 kDa. Although there are 400 amino acids that are different, shown in the results of sequence alignment between CAS and OSC, all steps in cycloartenol and lanosterol synthase are identical with the exception of the final deprotonation reaction. Cycloartenol synthase forms the cyclopropyl ring and abstracts a proton from C-19, whereas lanosterol synthase removes a different proton and forms lanosterol **(Fig. 1.14)**.



(3*S*)-2,3-Oxidosqualene    Protosteryl Cation    C-8 Cation    C-9 Cation

ERG7    CAS1

Lanosterol    Cycloartenol
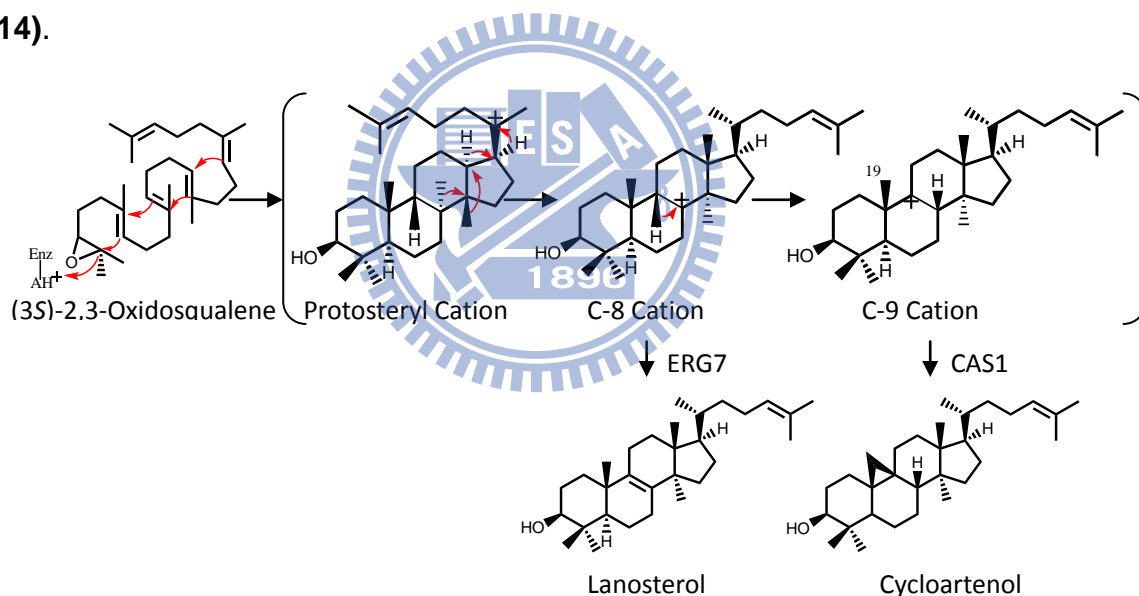
**Figure 1.14 The difference between cyclization mechanisms of lanosterol synthase and cycloartenol synthase.**

Phytosterols, such as campesterol and sitosterol, are biosynthesized from cycloartenol. Phytosterols, also called as plant sterols, are a group of naturally occurring steroid alcohols synthesized by plants. In addition to cholesterol-lowering effects, phytosterols have been suggested to possess anti-inflammatory, antibacterial, antifungal, antiulcerative, and antitumor activities.[31]

Cycloartenol synthase was first cloned from *Arabidopsis thaliana* (*Ath*CAS1), and

expressed and characterized in the yeast lanosterol synthase system in 1993.[32] Furthermore, because the cyclopropyl ring formation in the cycloartenol biosynthesis is thermodynamically unfavorable relative to that of the lanosterol formation, some of amino acid differences are probably specifically required for inducing cyclopropyl ring formation and excluding the formation of more energetically favored products by the cycloartenol synthase. The site-direct mutagenesis study of cycloartenol synthase (*Ath*CAS1) showed some important residues such as Tyr410, His477, and Ile481.[33] These residues are highly-conserved within cycloartenol synthase in many plant species, but they maintain Thr, Cys or Gln, and Val in the corresponding positions of ERG7 from animals and fungi **(Fig. 1.15)**. Speculation on this phenomenon, these residues may promote the formation of cyclopropyl rings within *Ath*CAS1; in other words, mutations at these positions may permit the lanosterol formation **(Table 1.1)**.

```
AthCAS1    QGYNG    412    TADHGWPISDCT    485
DdiCAS1    QGYNG    365    TVDHGWPISDCT    437
SceERG7    MGING    386    TKTQGYTVADCT    458
SpoERG7    RGING    381    NITQGYTVSDTT    453
HsaERG7    QGING    383    TLDCGWIVSDCT    457
RnoERG7    QGING    384    TLDCGWIVADCT    458
```

**Figure 1.15 Conservation pattern between CAS1 and ERG7**

Ile481 is conserved in all cycloartenol synthases, whereas Val is present in lanosterol synthase at this position. The γ-methyl of Ile481 might promote cycloartenol formation by preventing the rotation of the intermediate cation through steric interactions with C-2 and the two axial methyl groups at the A-ring. Removing the γ-methyl group with an Ile481Val substitution resulted in 25% lanosterol production in addition to production of cycloartenol and parkeol. In addition, Ile481 may also be involved in assisting in proper substrate folding, as well as for the cyclization reaction. Mutation of Ile481 to smaller residues such as Ala and Gly has led to achilleol A and camelliol C production **(Fig. 1.16)**.[34]

**Table 1.1 Product profiles of *Ath*CAS Ile481, Tyr410 and His477 mutants.**

| *Ath*CAS1<sup>mut</sup> | Cycloartenol | Lanosterol | Parkeol | 9β-lanosta-7,24-dien-3β-ol | Achilleol A | Camelliol C |
|---|---|---|---|---|---|---|
| Wild type | 99 | | 1 | | | |
| I481L | 83 | 1 | 16 | | | |
| I481V | 54 | 25 | 21 | | | |
| I481A | 12 | 54 | 15 | | 13 | 6 |
| I481G | 17 | 23 | 4 | | 44 | 12 |
| Y410T | | 65 | 2 | 33 | | |
| H477N | | 88 | 12 | | | |
| H477Q | | 22 | 73 | 5 | | |
| I481V/Y410T | | 75 | 1 | 24 | | |
| I481V/H477N/Y410T | | 78 | | 22 | | |
| I481V/H477Q/Y410T | | 78 | | 22 | | |
| I481V/H477N | | 99 | 1 | | | |
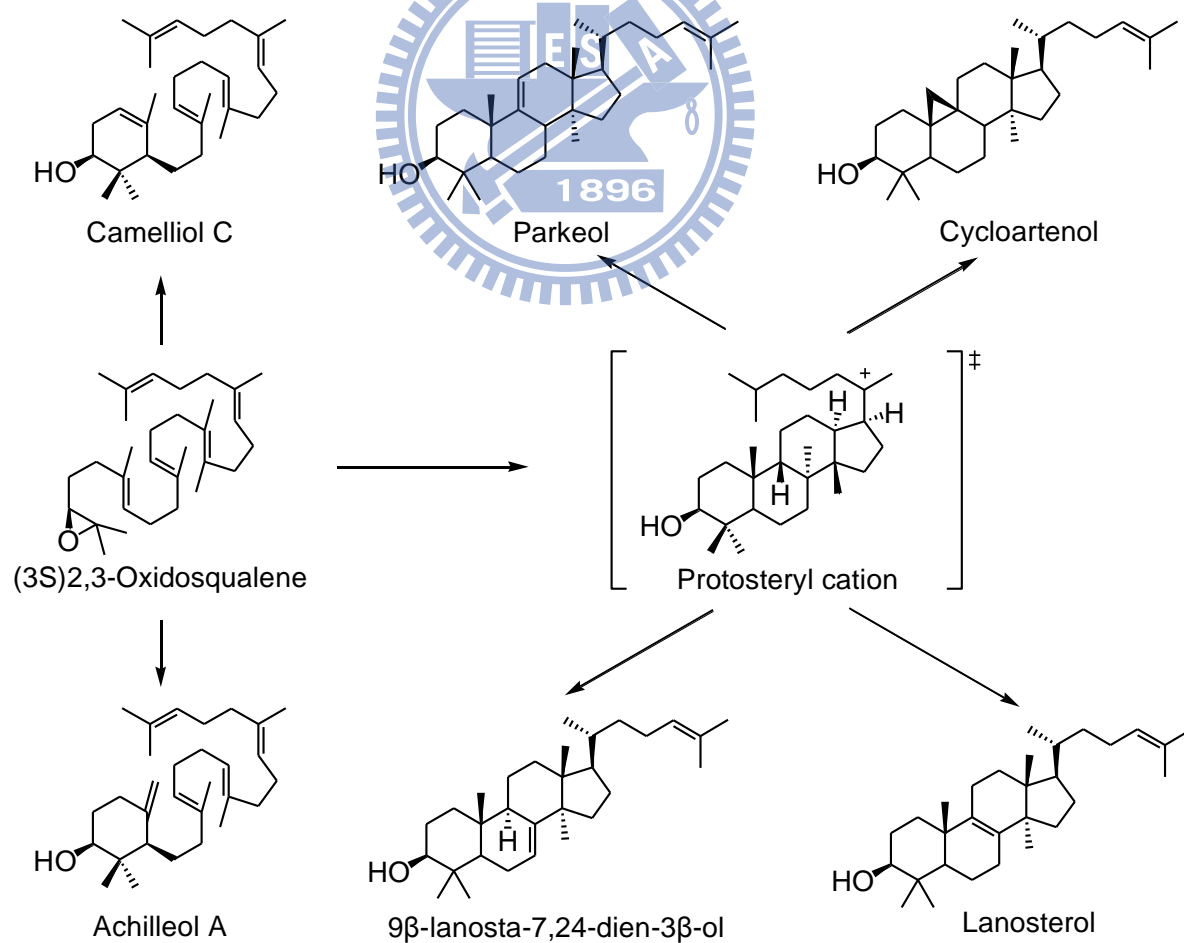


**Figure 1.16 Products formed by cycloartenol synthase mutants.**

Tyr410 and His257 participate in an H-bonding network positioned near the C-19 methyl group for the deprotonation reaction.[33] Tyr410 is present in all cycloartenol synthases, but animal and fungal oxidosqualene-lanosterol synthase maintain Thr at the corresponding position. The *Ath*CAS1[Tyr410Thr] mutant forms 65% lanosterol, along with 9β-lanosta-7,24-dien-3β-ol and parkeol. Removing the aromatic ring of Tyr410 decreases the steric bulk above the intermediate cation. Because the hydroxyl group in Thr is closer to its α-carbon than that in Tyr, the polar groups of Tyr410Thr, Tyr532, and His257 were repositioned in the Tyr410Thr mutant. This combination of steric and electronic changes abolishes the cycloartenol synthesis and allows deprotonation of C-8/C-9 lanosterol cation to form lanosterol, parkeol, and 9β-lanosta-7,24-dien-3β-ol.[35]

His477 is not in the active site, but is a second-sphere residue that affects the product profile through the interactions with the side chain of Tyr410.[33] His477 is strictly conserved in the known cycloartenol synthase, whereas lanosterol synthases maintain either Gln or Cys. The *Ath*CAS1[His477Gln] mutant has the polar functionality moved toward C-11, consequently resulting in more parkeol production than lanosterol. The *Ath*CAS1[His477Asn] mutant formed lanosterol by positioning the basic group near the C-9/C-8, but also produced parkeol due to a close enough distance to C-11.[36]

The double mutant of CAS1[I481V/ Y410T] formed lanosterol more accurately than either single mutant alone. However the triple mutant (His477Asn/Gln, Ile481Val, and Tyr410Thr) did not promote the lanosterol synthesis because the hydroxyl group of Thr is too distant to interact with the amide group of Asn or Gln residues. The His477Asn Ile481Val double mutant is the most accurate example for the enzyme mutation to generate lanosterol.[36]

## 1.3.5  β-amyrin synthase (βAS)

β-amyrin synthase originates from several plant species, such as *Pisum sativum* and *Panax ginseng*, and it is also a member of phytosterols biosynthesis pathway. The biosynthesis mechanism of β-amyrin is much different from that of lanosterol and cycloartenol. In the beginning, oxidosqualene is pre-folded into a chair-chair-chair conformation, and then forms the dammarenyl cation intermediate. Next, the D-ring expansion and E-ring cyclization occur, producing the 6-6-6-6-5 pentacyclic lupenyl cation. The lupenyl cation then converts to lupeol by deprotonation by lupeol synthase. But for β-amyrin synthase, the E-ring expands to continue the rearrangement cascade. Through the last deprotonation step, the β-amyrin is generated.
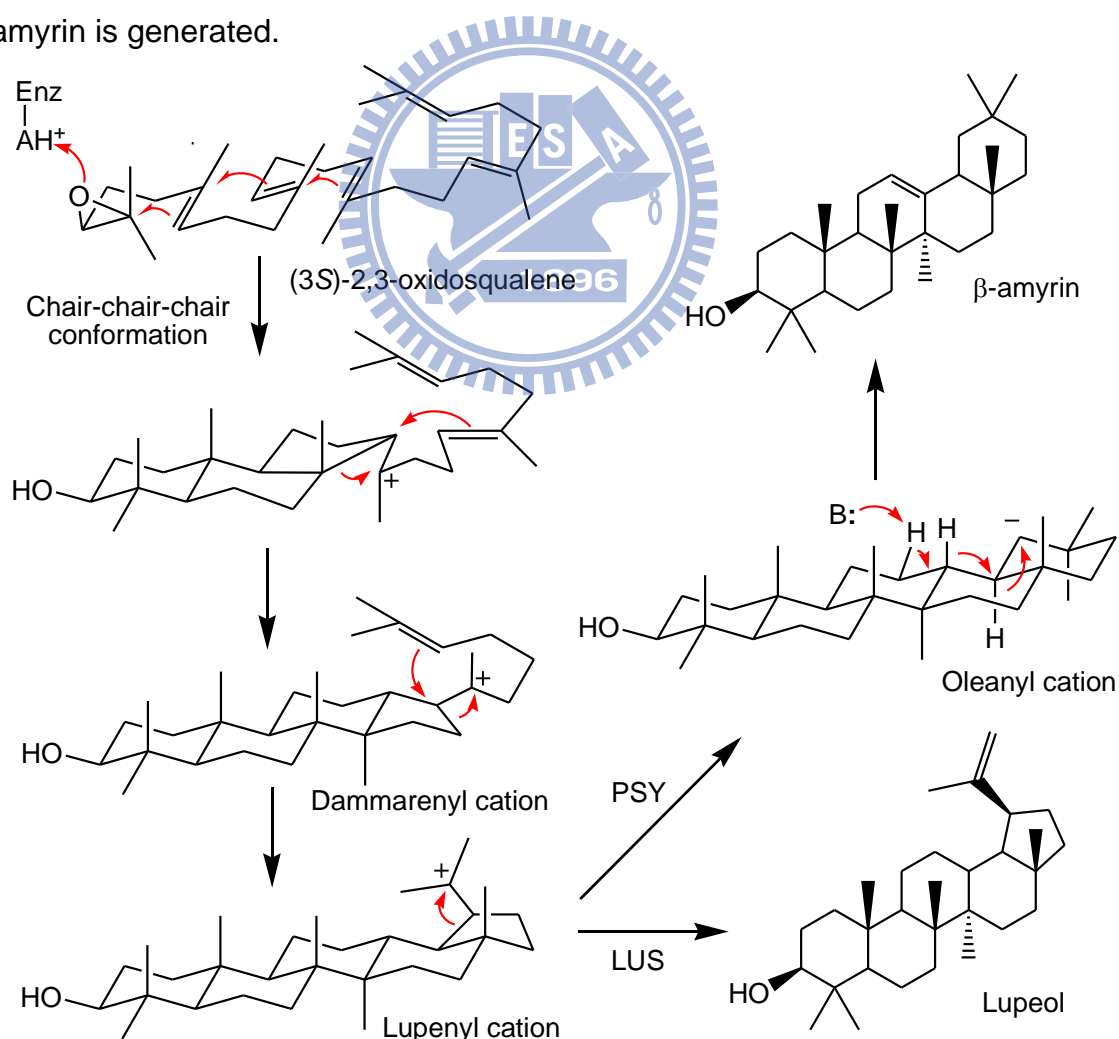
**Figure 1.17 Proposed mechanism of 2,3-oxidosqualene converted into β-amyrin and lupeol.**

Since the biogenetic isoprene rule proposed by Eschenmoser, Ruzicka, Arigoni, and Jeger in 1955,[27] the cyclization of (3$S$)-2,3-oxidosqualene into β-amyrin has fascinated organic chemists for over a half century. To investigate the catalytic motifs within cyclases that form the dammarenyl cation, the Ebizuba group first generated chimeras of the *A. thaliana* lupeol synthase and the *Panax ginseng* β-amyrin synthase.[37] They determined the function of the portions of cyclase by using a domain swapping strategy. It was observed that only relatively small portions of the protein can control the generation of lupeol or β-amyrin. One chimera in which only one fourth of the protein was β-amyrin sequence made four times as much β-amyrin as it did lupeol, and a mixed PCR method further confirmed the important region of chimeras. From an alignment analysis, it showed that the Trp259 within *Panax ginseng* β-amyrin synthase (PNY) and the Leu256 within *Olea europa* lupeol synthase (OEW) might control the product specificity.[38] Therefore, the authors constructed the PNY[Trp259Leu] and OEW[Leu256Trp] mutants and conducted the product analysis. Lupeol was twice as abundant as β-amyrin in the product profile of the PNY[Trp259Leu] mutant, whereas β-amyrin was the major product for the OEW[Leu256Trp] mutant. These results indicated that this position plays a critical role in directing either β-amyrin or lupeol formation. Furthermore, the authors created the PNY[Tyr261His] mutant and the experimental results showed that Tyr261 stabilizes one of the cationic intermediates formed after the dammarenyl cation.[22,37-38] In addition, the experimental results for *Pisum sativum* β-amyrin synthase (PSY) showed that the expansion of the D-ring could take place in the absence of the terminal double bond, so that the formation of anti-Markovnikov six-membered D-ring is independent of the terminal π-electrons. Thereby, the aromatic residues within the putative active site might play a crucial role for the ring expansion reaction.[21]

## 1.3.6　The amino acid sequence alignment

The amino acid sequence alignment of the enzyme cyclases could provide much information and led us understand these cyclases in depth. In evolutionary history, some highly-conserved residues indicated that they may play some specific function and it is necessary for the organisms. Therefore, it would be retained in various species. However, some other residues were not conserved or even deleted through the variation of evolution in many species. The information of these differences helped us to figure out the cyclized mechanism of enzyme cyclases. Moreover, their similar structures, stereoselectivity, and the catalytic mechanism were also investigated.[39] The relationship between the function and structure thus were deeply realized.

In order to understand the functional residues within the putative active site of triterpene cyclases, the program of Clustal W had been used to produce multiple sequence alignment of the following enzymes: *H. sapiens* ERG7: P48449, *S. cerevisiae* ERG7: P38604, *A. thaliana* CAS1: NP_178722, *P. sativum* PSY: BAA97558, *A. acidocaldarius* SHC: BAA25185. All of them were obtained from the Protein Data Bank (PDB) in NCBI, and the result of sequence alignment is shown below.

```
H.sapiens ERG7        MTEGTCLRRRGGPYKTEPATDLG--RWRLN-CERGRQTWTYLQDER--------AGREQT 49
S.cerevisiae ERG7     MTEFYSDTIG------LPKTDPR--LWRLRTDELGRESWEYLTPQQ--------AANDPP 44
A.thaliana CAS1       MWKLKIAEGGS-PWLRTTNNHVGRQFWEFDPNLGTPEDLAAVEEARKSFSDNRFVQKHSA 59
P.sativum PSY         MWRLKIAEGGNDPYLFSTNNFVGRQTWEYDPEAGSEEERAQVEEARRNFYNNRFEVKPCG 60
A.acidocaldarius SHC  ------------------------------------------------------------

H.sapiens ERG7        GLEAYALGLDTKNYFKDLPKAH------TAFEGALN----GMTFYVGLQAED-GHWTGDY 98
S.cerevisiae ERG7     STFTQWLLQDPK-FPQPHPERNKHSPDFSAFDACHN----GASFFKLLQEPDSGIFPCQY 99
A.thaliana CAS1       DLLMRLQFSRENLISPVLPQVKIEDTDDVTEEMVETTLKRGLDFYSTIQAHD-GHWPGDY 118
P.sativum PSY         DLLWRFQVLRENNFKQTIGGVKIEDEEEITYEKTTTTLRRGTHHLATLQTSD-GHWPAQI 119
A.acidocaldarius SHC  ---MAEQLVEAPAYARTLDRAV-------------------EYLLSCQKDE-GYWWGPL 36
```

```
H.sapiens ERG7        GGPLFLLPGLLITCHVAR---IPLPAGYREEIVRYLRSVQLP-DGGWGLHIEDKSTVFGT 154
S.cerevisiae ERG7     KGPMFMTIGYVAVNYIAG---IEIPEHERIELIRYIVNTAHPVDGGWGLHSVDKSTVFGT 156
A.thaliana CAS1       GGPMFLLPGLIITLSITGALNTVLSEQHKQEMRRYLYNHQNE-DGGWGLHIEGPSTMFGS 177
P.sativum PSY         AGPLFFMPPLVFCVYITGHLDSVFPPEHRKEILRYIYCHQNE-DGGWGLHIEGHSTMFCT 178
A.acidocaldarius SHC  LSNVTMEAEYVLLCHILDR----VDRDRMEKIRRYLLHEQRE-DGTWALYPGGPPDLDTT 91


H.sapiens ERG7        ALNYVSLRILGVGPDDP---DLVRARNILHKKGGAVAIPSWGKFWLAVLNVYSWEGLNTL 211
S.cerevisiae ERG7     VLNYVILRLLGLPKDHP---VCAKARSTLLRLGGAIGSPHWGKIWLSALNLYKWEGVNPA 213
A.thaliana CAS1       VLNYVTLRLLGEGPNDG-DGDMEKGRDWILNHGGATNITSWGKMWLSVLGAFEWSGNNPL 236
P.sativum PSY         ALNYICMRILGEGPDGGEDNACVRARNWIRQHGGVTHIPSWGKTWLSILGVFDWLGSNPM 238
A.acidocaldarius SHC  IEAYVALKYIGMSRDEE---PMQKALRFIQSQGGIESSRVFTRMWLALVGEYPWEKVPMV 148


H.sapiens ERG7        FPEMWLFPDWAPAHPSTLWCHCRQVYLPMSYCYAVRLSAAEDPLVQSLRQELYVEDFASI 271
S.cerevisiae ERG7     PPETWLLPYSLPMHPGRWWVHTRGVYIPVSYLSLVKFSCPMTPLLEELRNEIYTKPFDKI 273
A.thaliana CAS1       PPEIWLLPYFLPIHPGRMWCHCRMVYLPMSYLYGKRFVGPITSTVLSLRKELFTVPYHEV 296
P.sativum PSY         PPEFWILPSFLPMHPAKMWCYCRLVYMPMSYLYGKRFVGPITPLILQLREELHTEPYEKI 298
A.acidocaldarius SHC  PPEIMFLGKRMPLNIYEFGSWARATVVALSIVMSRQPVFPLPERARVP--ELYETDVPPR 206


H.sapiens ERG7        DWLAQRNNVAPDELYTPHSWLLRVVYALLNLYEHHHS------AHLRQRAVQKLYEHIVA 325
S.cerevisiae ERG7     NFSKNRNTVCGVDLYYPHSTTLNIANSLVVFYEKYLRN-----RFIYSLSKKKVYDLIKT 328
A.thaliana CAS1       NWNEARNLCAKEDLYYPHPLVQDILWASLHKIVEPVLMRWPG-ANLREKAIRTAIEHIHY 355
P.sativum PSY         NWTKTRHLCAKEDIYYPHPLIQDLIWDSLYIFTEPLLTRWPFNKLVRKRALEVTMKHIHY 358
A.acidocaldarius SHC  RRGAKGG-----------GGWIFDALDRALHGYQKLSVHP------FRRAAEIRALDWLLE 250
```

```
                                   V368  L372
H.sapiens ERG7        DDRFTKSISIGPISKTINMLVRWYVDGPASTAFQEHVSRIPDYLWMGLDGMKMQGTNGSQ 385
S.cerevisiae ERG7     ELQNTDSLCIAPVNQAFCALVTLIEEGVDSEAFQRLQYRFKDALFHGPQGMTIMGTNGVQ 388
A.thaliana CAS1       EDENTRYICIGPVNKVLNMLCCWVED-PNSEAFKLHLPRIHDFLWLAEDGMKMQGYNGSQ 414
P.sativum PSY         EDENSRYLTIGQVEKVLCMLACWVED-PNGDAFKKHIARVPDYLWISEDGMTMQSF-GSQ 416
A.acidocaldarius SHC  RQAGDGSWGGIQPPWFYALIALKILDMTQHPAFIKGWEGLELYGVELDYGGWMFQASISP 310
```

```
                       W416                                                  F472
H.sapiens ERG7        IWDTAFAIQALLEAGGHHRPEFSSCLQKAHEFLRLSQVP-DNPPDYQKYYRQMRKGGFSF 444
S.cerevisiae ERG7     TWDCAFAIQYFFVAGLAERPEFYNTIVSAYKFLCHAQF---DTECVPGSYRDKRKGAWGF 445
A.thaliana CAS1       LWDTGFAIQAILATNLVE--EYGPVLEKAHSFVKNSQVLEDCPGDLNYWYRHISKGAWPF 472
P.sativum PSY         BWDAGFAVQALLATNLIE--EIKPALAKGHDFIKKSQVTENPSGDFKSMHRHISKGSWTF 474
A.acidocaldarius SHC  VWDTGLAVLALRAAGLPAD---HDRLVKAGEWLLDRQIT--VPGDWAVKRPNLKPGGFAF 365
```

```
                                                                C484
                                                                 ↓
H.sapiens ERG7      STLDCGWIVSDCTAEALKAVLLLQEK--CPHVTEHIPRERLCDAVAVLLNMRNPD----G 498
S.cerevisiae ERG7   STKTQGYTVADCTAEAIKAIIMVKNSPVFSEVHHMISSERLFEGIDVLLNLQNIGSFEYG 505
A.thaliana CAS1     STADHGWPISDCTAEGLKAALLLSKVP-KAIVGEPIDAKRLYEAVNVIISLQNAD----G 527
P.sativum PSY       SDQDHGWQVSDCTAEGLKCCLLLSLLP-PEIVGEKMEPERLFDSVNLLLSLQSKK----G 529
A.acidocaldarius SHC QFDNVYYPDVDDTAVVVWALNTLRLPD------ERRRRDAMTKGFRWIVGMQSSN----G 415


                                             E548 F550 I553
                                              ↓    ↓    ↓
H.sapiens ERG7      GFATYETKRGGHLLELLNPSEVFGDIMIDYTYVECTSAVMQALKYFHKRFPEHRAAEIRE 558
S.cerevisiae ERG7   SFATYEKIKAPLAMETLNPAEVFGNIMVEYPYVECTSDSSVLGLTYFHKYF-DYRKEEIRT 564
A.thaliana CAS1     GLATYELTRSYPWLELINPAEVFGDIVIDYPYVECTSAAIQALISFRKLYPGHRKKEVDE 587
P.sativum PSY       GLAAWEPAGAQEWLELLNPTEFFADIVVEHEYVECTGSAIQALVLFKKLYPGHRKKEIEN 589
A.acidocaldarius SHC GWGAYDVDNTSDLPNHIPFCDFG--EVTDPPSEDVTAHVLECFG-------SFGYDDAWK 466


                                              W610       Y616
                                               ↓          ↓
H.sapiens ERG7      TLTQGLEFCRRQQRADGSWEGSWGVCFTYGTWFGLEAFACMGQTYRDGTACAEVSRACDF 618
S.cerevisiae ERG7   RIRIAIEFIKKSQLPDGSWYGSWGICFTYAGMFALEALHTVGETYEN---SSTVRKGCDF 621
A.thaliana CAS1     CIEKAVKFIESIQAADGSWYGSWAVCFTYGTWFGVKGLVAVGKTLKN---SPHVAKACEF 644
P.sativum PSY       FIFNAVRFLEDTQTEDGSWYGNWGVCFTYGSWFALGGLAAAGKTYTN---CAAIRKGVKF 646
A.acidocaldarius SHC VIRRAVEYLKREQKPDGSWFGRWGVNYLYGTGAVVSALKAVGIDTREP----YIQKALDW 522


H.sapiens ERG7      LLSRQMADGGWGEDFESCEERRYLQSA--QSQIHNTCWAMMGLMAVRHPDIE--AQERGV 674
S.cerevisiae ERG7   LVSKQMKDGGWGESMKSSELHSYVDSE--KSLVVQTAWALIALLFAEYPNKE--VIDRGI 677
A.thaliana CAS1     LLSKQQPSGGWGESYLSCQDKVYSNLDGNRSHVVNTAWAMLALIGAGQAEVDRKPLHRAA 704
P.sativum PSY       LLTTQREDGGWGESYLSSPKKIYVPLEGNRSNVVHTAWALMGLIHAGQSERDPTPLHRAA 706
A.acidocaldarius SHC VEQHQNPDGGWGEDCRSYEDPAYAGKG--ASTPSQTAWALMALIAGGRAESE--AARRGV 578


                                              F726 C730 I732 Y734 Y737
                                               ↓    ↓    ↓    ↓    ↓
H.sapiens ERG7      RCLLEKQLPNGDWPQENIAG-VFNKSCAISYTSYRNIFPIWALGRFSQLYPERALAGHP 732
S.cerevisiae ERG7   DLLKNRQEESGEWKFESVEG-VFNHSCAIEYPSYRFLFPIKALGMYSRAYETHTL---- 731
A.thaliana CAS1     RYLINAQMENGDFPQQEIMG-VFNRNCMITYAAYRNIFPIWALGEYRCQVLQQGE--- 759
P.sativum PSY       KLLINSQLEQGDWPQQEITG-VFMKNCMLHYPMYRDIYPLWALAEYRRRVPLP------ 758
A.acidocaldarius SHC QYLVETQRPDGGWDEPYYTGTGFPGDFYLGYTMYRHVFPTLALGRYKQAIERR------ 631
                                                    C703
```

**Figure 1.18 Amino acids alignment. The red words are the CAS1mut and the green one is ERG7C703 mutation.**

24

## 1.4    Research motive

The oxidosqualene cyclases family and their sterol products have fascinated scientists for more than half of a century. Not only biochemists, but also organic chemists and physical chemists, even pharmaceutical scientists and doctors are conducting research topic on this family of molecules. The goals of these studies are to understand the enzyme mechanisms, to make artificial enzymes to synthesize specific products, to find inhibitors to against bacteria or fungi, and to produce drugs to lower cholesterol levels or to kill cancer cells for various therapies.

The mechanism of the oxidosqualene cyclases activity involves cyclization and rearrangement. In fact, only one enzyme and one step is needed during the entire process of this amazing organic reaction. In addition, a few amino acid alterations could make a large stereochemical change on the product profiles. Currently, however, it is still troublesome to synthesize a compound when the processes are complicated, and involve a mass of chemicals. Studies on mechanisms in this area of chemistry could lead us to understand the relationship between the active-site amino acids and the appearances of products. In the future, synthesizing a complicated compound by using a few artificial enzymes is a goal worth achieving.

### 1.4.1    The study of Cys703 in *Sce*ERG7

In previous study,[40] the cysteine-modifying agent, 5,5-dithio-bis-(2-nitrobenzoic) acid (DTNB), was used to assess the possible role of cysteine residues in the enzymatic function of bovine liver OSC activity. The results show that there are two cysteine residues that play important roles in catalytic function or conformation in active site of ERG7.

Furthermore, in the sequence alignment of *Sce*ERG7, Cys703 is a highly-conserved residue in the oxidosqualene cyclases family. By homology modeling, it is a secondary sphere residue in the active-site, where the Phe699 locates between Cys703 and the substrate. The minimum distance from Cys703 to the lanosterol molecule within the *Sce*ERG7 modeling structure is 7.01 Å, while the distance between Cys703 and Phe699 is only 3.28 Å. Therefore, the mutation on Cys703 might change the situation of Phe699, and influence the mechanism of cyclization and rearrangement **(Fig. 1.19)**. Some further studies showed the importance of second-sphere residues. The best example is the His477 within *Ath*CAS1, which is hydrogen bonded to Tyr410, thus it is essential for cycloartenol biosynthesis.[33]
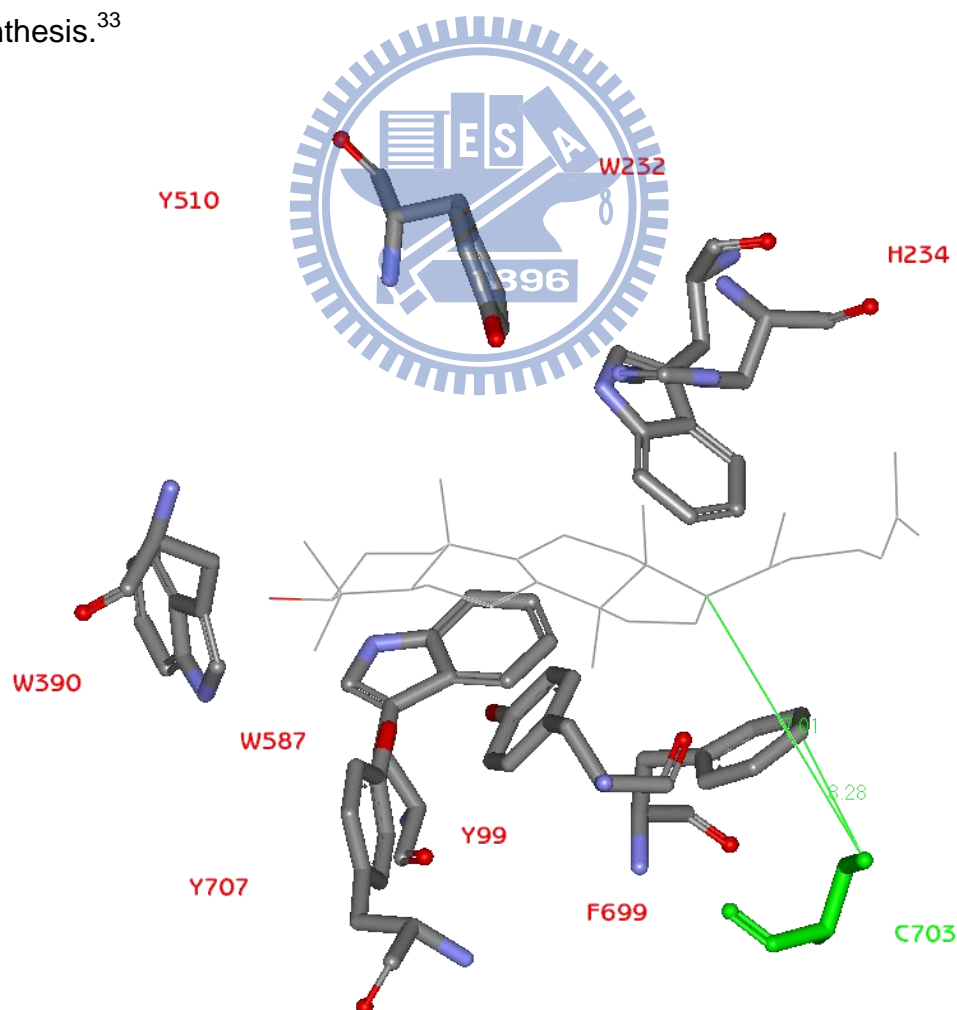


**Figure 1.19 The position of Cys703 in the active-site within *Sce*ERG7.**

According to the griffin aromatic hypothesis, the role of aromatic residues is considered to stabilize the highly-energy cation intermediate. The aromatic residues, which are within the putative active site, include Tyr99, Trp232, His234, Trp390, Trp443, Phe445, Tyr510, Phe699, and Tyr707. Among them, Phe699 affects the C-17 cation directly. The mutation on the Phe699 residue could produce many truncated compounds that reflect the unstable actuality of the C-17 cation. Therefore, the mutation on the Cys703 residue might indirectly influence the Phe699 residue to cause similar results.

On the other hand, the argument regarding the B-chair/boat ring and the 17α/17β mechanistic transitions has occurred lately in evolutionary history.[41] The multiple products of oxidosqualene cyclases including the B-chair ring with the 17α/17β skeleton and B-boat ring with the 17β structure were isolated. Fascinatingly, no B-boat compounds with the 17α skeleton have found been in nature.[42] So the method could be a means to understand the stereochemistry of enzymatic control. Through the mutation on the residue Cys703 within *Sce*ERG7, the steric effect close to the C-17 cation might change. By analyzing its coresponding products, the relationship of structure-function might be understood in better detail.

## 1.4.2 The study of CAS1 in *A. thaliana* and PSY in *P. sativum*

To understand the entire stereochemical mechanism of oxidosqualene cyclases, not only the information acquired from the mutation on Cys703 within *Sce*ERG7, but also the information by comparing the similarities and dissimilarities between cycloartenol synthase (CAS) and β-amyrin synthase (βAS) are needed. Either the CAS or βAS are found in higher plants. Some species, such as *Arabidopsis thaliana*, contain both of CAS and βAS, with distinct stero-chemical control. Many differences exist between CAS and βAS, even in the same species. CAS triggers the substrate into the chair-boat-chair conformation, forming the protosteryl cation intermediate and producing the final tetracyclic compound. βAS catalyzes the OS to go though the chair-chair-chair dammarenyl cation to form the pentacyclic product. In addition, there are some mutational studies between lupeol synthase and β-amyrin synthase as mentioned earlier, to illustrate their stero-chemical selectivity.

On the other hand, detailed information about amino acids in the active-site is critical to understand the whole mechanism of one enzyme. Just like the lanosterol cyclase from *S. cerevisiae*, the complete alanine-scanning of the active-site had been done by our laboratory. Our data indicated that the residue plays an important role in catalytic reaction of the enzyme, while an amino acid mutated to alanine produced novel products or lost the enzyme activity dramatically.

According to the view as mentioned above, to construct a complete site-directed alanine-scanning experiment is necessary. So based on the previous study[19], many important residues were chosen in the SHC active-site. Fifteen amino acids from the SHC active-site had been chosen to find their corresponding residues in *Ath*CAS1 and *Psa*PSY, then the change of the product profile was analyzed in each mutant **(Fig. 1.20)**. The residues in CAS1 (or PSY) are V368(V371), L372(L374), W416(W418), F472(F474), C484(C486), E548(E550), F550(F552),

I553(I555), W610(W612), Y616(Y618), F726(F728), C730(C732), I732(L734), Y734(Y736) and Y737(Y739). By mutating the residues, more information could be obtained. Based on the given information, it is possible to preliminarily predict the stereochemical mechanism of enzyme-mediated cyclization, to propose a foundation for the further studies.
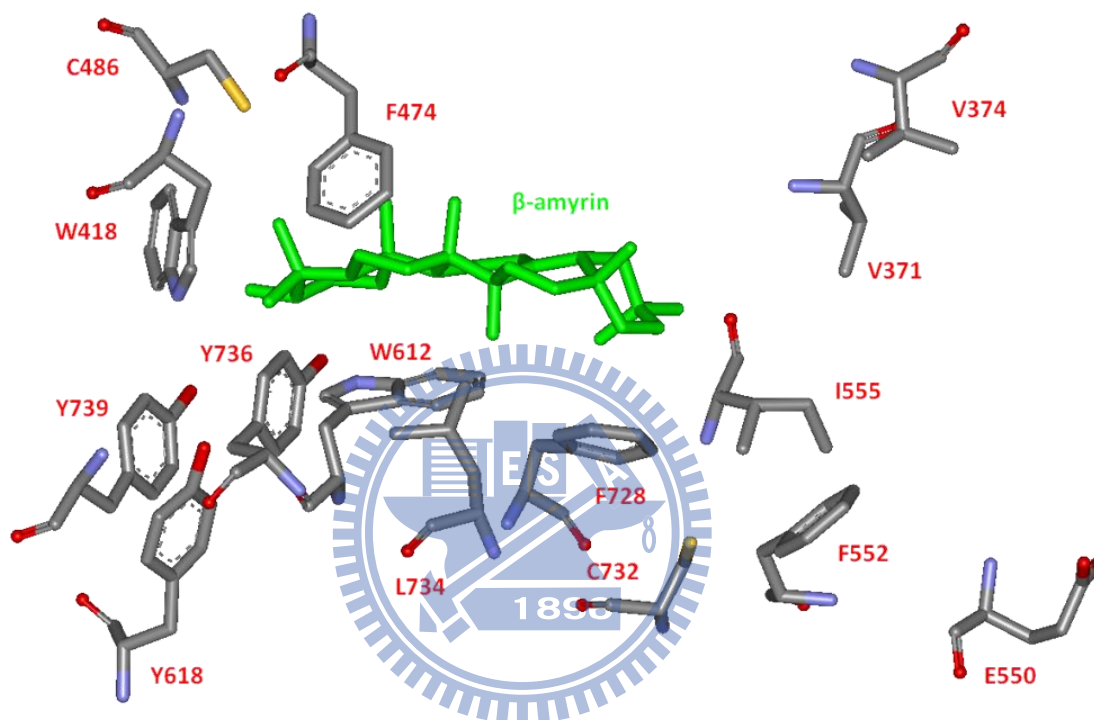


**Figure 1.20 The alanine-scanning mutation position in the active-site of β-amyrin synthase within *Pisum sativum*.**

# Chapter 2   Materials and methods

## 2.1   Materials

### 2.1.1   Chemicals, reagents and kits

**Purchase from Sigma:**

Acetic anhydride

Adenine

Ampicillin sulfate

D-Sorbitol

Ergosterol

Glucose

Histidine

Lysine

Methionine

Pyridine

Tryptophan

Uracil

**Purchase from Merck:**

95%Ethanol

Acetic acid

Acetone

Anisaldehyde

Dichloromethane

Ether

Ethyl acetate

Glycerol

Hemin Chloride

Hexane

Methanol

Potassium hydroxide

Pyrogallol

Silica gel

Sodium sulfate

Sulfonic Acid

TLC plate

Tween 80


## Purchase from USB:

Agarose-LE

Bromophenol blue


## Purchase from DIFCO:

Bacto$^{TM}$ Agar

LB Broth, Miller

Trypton

Yeast Extract

Yeast Nitrogen Base w/o amino acid


## Purchase from other companies:

BigDye$^{®}$ Teminator v3.1 Cycle Sequencing Kit (Applied Biosystems)

Dimethyl sulfoxide (MP Biomedicals)

DNA 10Kb Ladder (Bio Basic Inc., Tanwan)

dNTP Set, 100mM Solutions (GE Healthcare)

G418 (Gibco)

GFX<sup>TM</sup> PCR DNA and Gel Band Purification Kit (GE Healthcare)

Plasmid Miniprep Purification Kit (GeneMark)

Primers (Bio Basic Inc.)

QuikChange Site-Directed Mutagenesis Kit (Stratagene Inc., La Jolla, CA)

Restriction enzymes (New England BioLabs Inc.)

SYBR<sup>®</sup> Green I (Roche)

## 2.1.2 Bacterial, yeast strains and vectors

*Escherichia coli* XL1-Blue (Novagen)

TKW14C2 (a yeast stain, MATa or MATα ERG7Δ:: LEU2 *ade*2-101 *his*3-Δ200 *leu2*-Δ1

*lys*2-801 *trp1*-Δ63 *ura3*-52 *hem1*Δ::Kan<sup>R</sup>)

Vector pRS313 (a shuttle vector with selection marker *His3*, New England BioLabs)

Vector pRS314 (a shuttle vector with selection marker *Trp1*, New England BioLabs)

## 2.1.3 Equipments

ABI PRISM® 3100 Genetic Analyzer (Applied Biosystems)

Allegra<sup>TM</sup> 21R Centrifuge (Beckman Coulter)

Avanti® J0E Centrifuge (Beckman Coulter)

Centrifuges 5415R (eppendorf)

Colling Circulator Bath Model B401L (Firstek Scientific)

DU 7500 UV-Vis Spectrophotometer (Beckman Coulter)

Durabath<sup>TM</sup> Water Bath (Baxter)

Electrophoresis Power Supply EPS 301 (GE healthcare)

GeneAmp® PCR System 9700 Thermal Cycler (Applied Biosystems)

Hoefer® HE 33 Mini Horizontal Submarine Unit (GE Healthcare)

Kodak Electrophoresis Documentation an Analysis System 120 (Kodak)

Orbital Shaking Incubator Model-S302R (Firstek Scintific)

Pulse Controller (BioRad)

Rotary Vaccum Evaporator N-N Series (EYELA)

Steritop$^{TM}$ 0.22μm Filter Unit (Millipore)


## 2.1.4    Solutions and mediums

**Ampicillin stock solution (100 mg/mL)**

Dissolve 1 g ampicillin sulfate in 10 mL ddH$_2$O. Filter through 0.22 μm pore size

filter and store at -20 °C.


**50X TAE buffer**

Dissolve Tris base 242 g, acetic acid 57.1 ml, and 0.5 M EDTA in 1 L dH$_2$O and

adjust to pH 8.5.


**50X ALTHMU solution**

1 g Adeine, 1.5 g Lysine, 1 g Tryptophan,, 1 g Hisidine, 1 g Methonine, 1 g Uracil

dissolved in 500 ml dH$_2$O and sterilized.


**50X ALHMU solution**

1 g Adeine, 1.5 g Lysine, 1 g Hisidine, 1 g Methonine, 1 g Uracil dissolved in 500

ml dH$_2$O and sterilized.

**50X ALTMU solution**

1 g Adeine, 1.5 g Lysine, 1 g Tryptophan, 1 g Methonine, 1 g Uracil dissolved in 500 ml dH$_2$O and sterilized.

**50% Glucose solution**

500 g glucose dissolved in 1 L dH$_2$O and sterilized.

**80% Glycerol solution**

80 mL glycerol added in 20 mL dH$_2$O and sterilized.

**LB medium**

25 g LB Broth dissolved in 1 L dH$_2$O and sterilized. Store at 4 °C.

**LB plate**

25 g LB Broth and 20 g Bacto$^{TM}$ Agar dissolved in 1 L dH$_2$O and sterilized. The sterile LB agar was poured and dispersed in Petri dishes before it coagulates. Store at 4 °C.

**G418 stock solution (1g/mL)**

Dissolve 500 mg G418 in 500 µl sterile dH$_2$O. Store in darkness at 4 °C.

**YNB medium**

6.7 g Yeast nitrogen base dissolved in 1 L dH$_2$O and sterilized.

**1 M sorbitol solution**

172.2 g D-sorbitol dissolved in 500 ml dH$_2$O and sterilized. Store at 4 °C.

**Hemin solution**

0.5 g hemin chloride dissolved in 250 ml 0.2 M sodium hydroxide and thus mixes it with 250 ml 95% alcohol in aseptic condition. Store it in darkness at 4 °C.

**Ergosterol supplement solution**

1 g Ergosterol dissolved in 250 ml 95% alcohol. Then mixed with 250 ml Tween 80 in aseptic condition. Store in darkness at 4 °C.

**ALHMU (ALTMU) electorporation plate**

0.67 g yeast nitrogen base, 2 g Bacto$^{TM}$ Agar and 36.5 g D-sorbitol dissolved in 100 ml dH$_2$O and sterilized. Add 2 ml 50X ALHMU (ALTMU) solution, 4 ml 50% glucose solution, 2 ml hemin solution, 2 ml ergosterol solution when cool. Then the mixture was poured and dispersed in Petri dishes before it coagulates. Store it in darkness at 4 °C.
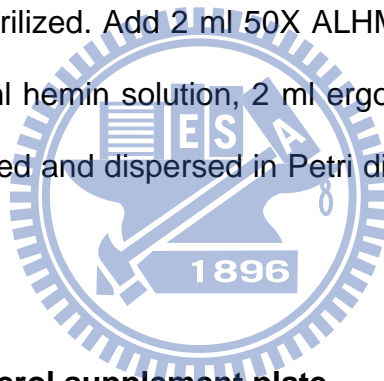
**ALHMU (ALTMU) ergosterol supplement plate**

0.67 g yeast nitrogen base, 2 g Bacto$^{TM}$ Agar dissolved in 100 ml dH$_2$O and sterilized. Add 2 ml 50X ALHMU (ALTMU) solution, 4 ml 50% glucose solution, 2 ml hemin solution when cool. Then mixed with and without 2 ml ergosterol solution, respectively. The mixture was poured and dispersed in Petri dishes before it coagulates. Store it in darkness at 4 °C.

**YNB liquid culture medium**

100 ml YNB medium contains 2 ml 50X ALTHMU, ALHMU or ALTMU solution, 4 ml 50% glucose solution, 2 ml hemin solution and 2 ml ergosterol solution

**20% EA developing solution**

Add 20 ml ethyl acetate to 80 ml hexane and mixing.

**TLC staining solution**

40 ml of conc. $H_2SO_4$ added (slowly!) into ethanol 800 ml, followed by acetic acid

12 ml and anisaldehyde 16 ml.

**5X sequencing buffer**

Dissolve 4.85 g Tris base and 0.203 g $MgCl_2$ in 100 ml $dH_2O$ and adjust to pH 9.

Store at 4 °C.

**10X SYBR Green solution**

10000X SYBR Green diluted to 10X with DMSO. Store in darkness at -20 °C.

**6X DNA loading dye**

0.25% bromophenol blue and 30% glycerol dissolved in $ddH_2O$. Store at -20 °C.

## 2.2 Methods

### 2.2.1 The construction of recombinant plasmids

The ERG7 and βAS mutations were performed using the QuikChange site-directed mutagenesis kit. The CAS1 mutations were constructed already in our laboratory.

### 2.2.1.1 Design primers:

For the ERG7$^{C703X}$ mutations:

**YCC-YOSC-C703IKMNRST-MfeI-1**

5'- CAA CCA CTC T**AN S**g<u>C AAT Cg</u>A ATA CCC AAg- 3'

**YCC-YOSC-C703IKMNRST-MfeI-2**

5'- CTT ggg TAT T<u>Cg ATT g</u>C**S NT**A gAg Tgg TTg- 3'

**YCC-YOSC-C703CFLSWY-MfeI-1**

5'- CAA CCA CTC T**TN S**g<u>C AAT Cg</u>A ATA CCC AAg- 3'

**YCC-YOSC-C703CFLSWY-MfeI-2**

5'- CTT ggg TAT T<u>Cg ATT g</u>C**S NA**A gAg Tgg TTg- 3'

**YCC-YOSC-C703HLPQR-MfeI-1**

5'- CAA CCA CTC T**CN S**g<u>C AAT Cg</u>A ATA CCC AAg- 3'

**YCC-YOSC-C703HLPQR-MfeI-2**

5'- CTT ggg TAT T<u>Cg ATT g</u>C**S Ng**A gAg Tgg TTg- 3'

**YCC-YOSC-C703ADEGV-MfeI-1**

5'- CAA CCA CTC T**gN S**g<u>C AAT Cg</u>A ATA CCC AAg- 3'

37

**YCC-YOSC-C703ADEGV-MfeI-2**

5'- CTT ggg TAT T<u>Cg ATT g</u>C**S NC**A gAg Tgg TTg- 3'


For the ERG7$^{F699X/C703I}$ double mutations:

**YCC-YOSC-C703I-disPvuIIforF699X-1**

5'- CCA CAg CAT TgC AAT TgA ATA C- 3'

**YCC-YOSC-C703I-disPvuIIforF699X-2**

5'- gTA TTC AAT TgC AAT gCT gTg g- 3'


For the βAS alanine scaning mutations:

**YCC-PSY-V371A-MfeI-1**

5'-CgA TAC CTT ACA ATT ggC TgT gCg gAA AAg-3'

**YCC-PSY-V371A-MfeI-2**

5'-CTT TTC CgC ACA gCC AAT TgT AAg gTA TCg-3'


**YCC-PSY-V374A-MfeI-1**

5'-CTT ACA ATT ggC TgT gTg gAA AAg gCT TTA Tg-3'

**YCC-PSY-V374A-MfeI-2**

5'-CAT AAA gCC TTT TCC ACA CAg CCA ATT gTA Ag-3'


**YCC-PSY-W418A-HindIII-1**

5'-CAA gAA gCg gAT gCT ggT TTT gCC gTT CAg gCT TTg-3'

**YCC-PSY-W418A-HindIII-2**

5'-CAA AgC CTg AAC ggC AAA ACC AgC ATC CgC TTC TTg-3'

**YCC-PSY-F474A-NcoI-1**

5'-gTg gAC CgC CTC TgA TCA AgA CCA Tgg ATg-3'

**YCC-PSY-F474A-NcoI-2**

5'-CAT CCA Tgg TCT TgA TCA gAg gCg gTC CAC -3'


**YCC-PSY-C486A-NcoI-1**

5'-gAC CAT ggA Tgg CAA gTT TCT gAT gCC ACC gC-3'

**YCC-PSY-C486A-NcoI-2**

5'-gCg gTg gCA TCA gAA ACT TgC CAT CCA Tgg TC-3'


**YCC-PSY-E550A-BglI-1**

5'-CTA CTC AAT CCT ACA gCC TTT TTg gCg gAC-3'

**YCC-PSY-E550A-BglI-2**

5'-gTC CgC CAA AAA ggC TgT Agg ATT gAg TAg-3'
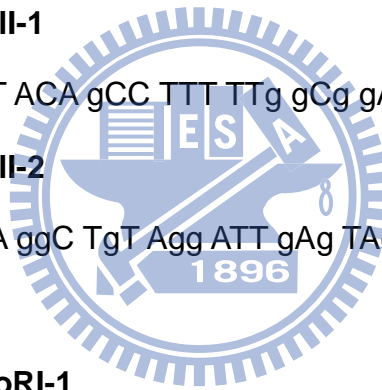

**YCC-PSY-F552A-EcoRI-1**

5'-CTC AAT CCT ACA gAA TTC gCT gCg gAC ATT g-3'

**YCC-PSY-F552A-EcoRI-2**

5'-CAA TgT CCg CAg CgA ATT CTg Tag gAT TgA g-3'


**YCC-PSY-I555A-EcoRI-1**

5'-CCT ACA gAA TTC TTT gCg gAC gCT gTT gTT g-3'

**YCC-PSY-I555A-EcoRI-2**

5'-CAA CAA CAg CgT CCg CAA AgA ATT CTg TAg g-3'

**YCC-PSY-W612A-NdeI-1**

5'-ggA AAC gCg ggA gTT TgC TTT ACA TAT ggC-3'

**YCC-PSY-W612A-NdeI-2**

5'-gCC ATA TgT AAA gCA AAC TCC CgC gTT TCC-3'

**YCC-PSY-Y618A-PvuII-1**

5'-gCT TTA Cgg CTg gCA gCT ggT TCg CTC TTg-3'

**YCC-PSY-Y618A-PvuII-2**

5'-CAA gAg CgA ACC AgC TgC CAg CCg TAA AgC-3'

**YCC-PSY-F728A-BspHI-1**

5'-gAA ATC ACA ggA gTA gCC ATg AAA AAT TgC-3'

**YCC-PSY-F728A-BspHI-2**

5'-gCA ATT TTT CAT ggC TAC TCC TgT gAT TTC-3'

**YCC-PSY-C732A-BspHI-1**

5'-ggA gTA TTT ATg AAA AAT gCC ATg TTg CAC-3'

**YCC-PSY-C732A-BspHI-2**

5'-gTg CAA CAT ggC ATT TTT CAT AAA TAC TCC-3'

**YCC-PSY-Y736A-NruI-1**

5'-gTT gCA CgC TCC AAT gTA TCg CgA TAT ATA TC-3'

**YCC-PSY-Y736A-NruI-2**

5'-gAT ATA TAT CgC gAT ACA TTg gAg CgT gCA AC-3'

**YCC-PSY-Y739A-NruI-1**

5'-CAC TAT CCA ATg gCT CgC gAT ATA TAT CCA C-3'

**YCC-PSY-Y739A-NruI-2**

5'-gTg gAT ATA TAT CgC gAg CCA TTg gAT AgT g-3'

## 2.2.1.2 QuickChange PCR:

**Table 2.1 QuickChange Site-Directed Mutagenesis Kit PCR composition**

| Reagent | Volume (µl) | Total |
|---------|-------------|-------|
| Primer1 (1000 ng/µl) | 0.5 | |
| Primer2 (1000 ng/µl) | 0.5 | |
| Template | 0.5 | |
| dNTP (10 mM) | 1.6 | 20 |
| *Pfu* II buffer | 2 | |
| *Pfu* II polymerase | 0.4 | |
| DDW | 14.5 | |

**Table 2.2 QuickChange Site-Directed Mutagenesis PCR program**

| Segment | Cycles | Temperature (°C) | Time |
|---------|--------|------------------|------|
| 1 | 1 | 95 | 2 min |
| 2 | 25 | 95 | 30 sec |
| | | 52 | 1min |
| | | 68 | 8min |
| 3 | 1 | 4 | ∞ |

## 2.2.1.3 *Dpn* I digest parental DNA template:

Add 1µl *Dpn* I and 1 µl 10X NEB buffer to 8 µl PCR products. The digested reaction was incubated at 37 °C for 3 hours to digest the parental supercoiled DNA.

## 2.2.1.4 Transformation into XL1-Blue and enzyme digestion:

The digested QuickChange products were added into 100 µl *E. coli* XL1-Blue

competent cells of each reaction and incubated on ice for 20 min. The cells were transformed by heat shock methods for 1min at 42 °C, following 1 min on ice. Then the cells were transferred into 1ml Luria-Bertani (LB) medium immediately and then shaken in 200 rpm for 1 hour at 37 °C incubator. Then, the cells were centrifuged at 6,000 rpm for 1 min and propagated on LB plate containing 100 µg/ml ampicillin. Incubate these plates 16 hr at 37 °C. Pick the colonies and culture in 3 ml LB medium containing 100 µg/ml ampicillin overnight at 37 °C. The plasmids were isolated by Plasmid Miniprep Purification Kit, according to the manufacturer instructions. The plasmids were then digested with restricion enzymes respectively to confirm the presence of the mutations.

## 2.2.1.5 Sequencing analysis

The exact amino acid substitutions were determined by sequencing of the DNA using ABI PRISM 3100 auto-sequencer. Nucleotide sequencing was performed using the dideoxynucleotide chain-termination method with only one forward of reverse primers. Sequencing reactions were carried out with BigDye® Terminator v3.1 Cycle Sequencing Kit, according to the manufacturer protocol. Briefly, each of sample was performed with 1 µl each forward or reverse primer, 2 µl plasmid DNA, 3 µl 5X sequencing buffer, 0.5 µl premix and ddH$_2$O to create a final volume of 20 µl. Each of the reaction was performed on the ABI PRISM® 3100 Genetic Analyzer, following the manufacturer's guidelines.

## 2.2.2  Transformation and Genetic selections ERG7 mutants
## 2.2.2.1 Preparation of competent cell TKW14C2

Pick the yeast TKW14C2 stock into the 3 ml ALTHMU YNB liquid culture medium and then incubated at 30 °C for about five days. When the cell grew well,

transferred it into 100 ml ALTHMU YNB liquid culture medium and incubated at 30 °C for 16-18 hours. After $OD_{600}$ of it reaches 1.0~1.5, the cells were centrifuged to collect at 3000 rpm, 10 min at 4 °C and the supernatant was discarded. Add about 45 ml aseptic $ddH_2O$ to resuspend the pellet and centrifuge it at 3000 rpm, 10 min at 4 °C and then repeated two times. Next, adding 25 ml of 1 M D-sorbitol solution to resuspend the pellet and centrifuge it at the same condition. Finally, add n×50 μL (n is the number of samples) 1 M D-sorbitol into the pellet and resuspend it gentlemanly on ice for about 5 min. The volume of 50 μl competent cells was added into each of 1.5 ml microtube with 5 μl recombinant plasmids, respectively.

## 2.2.2.2 Transformation of mutated plasmid into TKW14C2

The mutated plasmids were transformed into TKW14C2, an ERG7-deficient yeast strain, by electroporation using a GenPulser with Pulse Controller (BioRad). At beginning, pipette total of competent cell with plasmid DNA onto drop and flick cuvette to settle DNA and yeast cells mixture into bottom of cuvette. Then set the conditions for transformation according to strains. For TKW14C2 cells, use 1.5k volt and the time constant should be 3-4 seconds. After electroporation, immediately add 500 μl of D-sorbitol solution into the cuvette. Aliquots of 120 μl of each culture were plated onto ALHMU or ALTMU electroporation plates, and incubated them for five days to select for the presence of plasmids.

## 2.2.2.3 Ergosterol supplement

Several colonies from each of plate were picked to reselect on two ergosterol supplement plates. The transformants were incubated three to five days at 30 °C. Ergosterol supplement is a selection marker for functional complementation of cyclase in ERG7 mutants.

## 2.2.3　Extracting lipids and characterizing mutant product profiles

### 2.2.3.1 Cell culture and extraction

In the small scale incubation, the mutant transformants were grown in the 2.5 L YNB liquid culture medium at 30 °C with 200 rpm shaking for five days. The cells were harvested by centrifugation at 6000 rpm for 10 minutes. The pellets were resuspending in the solution containing 100 ml ethanol, 100 ml 30% KOH, and 0.2 g pyrogallol. This reaction was refluxed at 110 °C for 3 hours. The hydrolysate was extracted three times with total 600 ml petroleum ether, the organic phase were collected and dehydrated by sodium sulfate and concentrated using a rotary evaporator. The small amount of nonsaponofiable lipid was dissolved in Acetone.

### 2.2.3.2 Silica gel column chromatography

The extract was fractionated by silica gel column chromatography using a 19:1 hexane/ethyl acetate mixture. Each of fractions was spotted on the thin-layer chromatography which developed with 4:1 hexane/ethyl acetate and the TLC plates were subjected to the TLC staining solution and heated until the patterns appeared. According the TLC results, the fractions can be divided into five regions: OS, LA up, LA, LA down, and Erg. The fractions of LA up, LA, and LA down sections were performed on GC/MS analysis for examination the triterpene products with a molecule mass of $m/z$ = 426.

### 2.2.3.3 GC-MS column chromatography condition

GC analyses were performed with a Hewlett-Packard model 5890 series II or Agilent 6890N chromatography equipped with a DB-5 column (30 m x 0.25 mm I.D., 0.25 μm film; oven gradient at 50 °C for 2 min, and then 20 °C per min until 300 °C,

held at 300 °C for 20 min, 300 °C injector; 250 °C interface; 1/40 split ratio using helium carrier gas at 13 psi column head pressure). GC/MS was performed on a Hewlett-Packard model 5890 II GC (J &W DB-5MS column, 30 m x 0.25 mm I.D., 0.25 μm film; oven 280 °C, injector 270 °C, GC-MS transfer line: 280 °C) coupled to a TRIO-2000 micromass spectrometer.

## 2.2.4   Molecular modeling

Molecular-modeling studies were performed, using the DiscoveryStudio program with the X-ray structure of lanosterol-complexed human OSC as the template. Then using GOLD program for ligand docking, finally using SYBYL program for minimum of the energy. The homologous model structure would be obtained with optimum condition. All of the molecular modeling softwares are provide by National Center for High-Performance Computing (NCHC) institution.
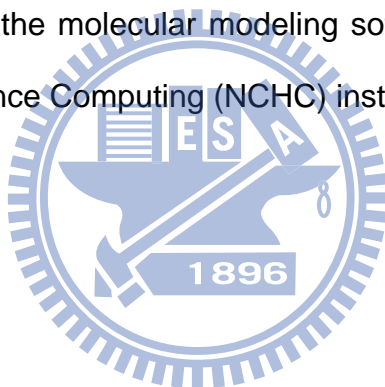
# Chapter 3　Results and Discussion

## 3.1　Functional analysis of *S. cerevisiae* ERG7

In the previous study, cysteine residues played important roles in the OSC active site of catalytic function or conformation. Furthermore, the residue Cys703 in the putative active site cavity of oxidosqualene-lanosterol cyclase is highly conserved. Although Cys703 is not close to the substrate, there are some examples that second-sphere residues may affect the first-sphere amino acid, and subsequently cause product diversity in cycloartenol biosynthesis pathway.

For these reasons, the residue Cys703 was subjected to site-saturated mutagenesis and product characterization to investigate the mutational effects on enzyme catalysis and product profile.

## 3.1.1　Site-saturated mutagenesis of Cys703

The saturated mutations of Cys703 in ERG7 from *Sacchromyces cerevisiae* were constructed employing QuikChange Site-Directed Mutagenesis kit, and mapped by restriction enzyme *Mfe* I. All mutated plasmids were confirmed by DNA sequencing via the ABI PRISM 3100 DNA sequencer.

The recombinant plasmids were electroporated into the yeast TKW14C2 strain (MATa/α ERG7Δ::LEU2 *hem1*Δ::G418 *ade*2-101 *his*3-Δ200 *leu*2-Δ1 *lys*2-801 *trp1*-Δ63 *ura3*-52) for the *in vivo* analysis. The yeast system, TKW14C2 is a CBY57-derived *hem1 erg7* double-knockout mutant and is only viable when it is supplied with ergosterol from ERG7^C703X mutants **(Fig. 3.1)**.

From the genetic selection among *S. cerevisiae* ERG7^C703X mutants, the C703X (X= G, V, I, S, T, N, D, H) complemented the ERG7 disruption strain, TKW14C2 in

the absence of exogenous ergosterol, while the other mutants (X=A, L, F, Y, W, E, Q, K, R, P, M) failed to complement **(Table 3.1)**. These results suggest that the different side chain substitution of C703 will influence the enzymatic activity, and abolish the cyclization process of oxidosqualene.
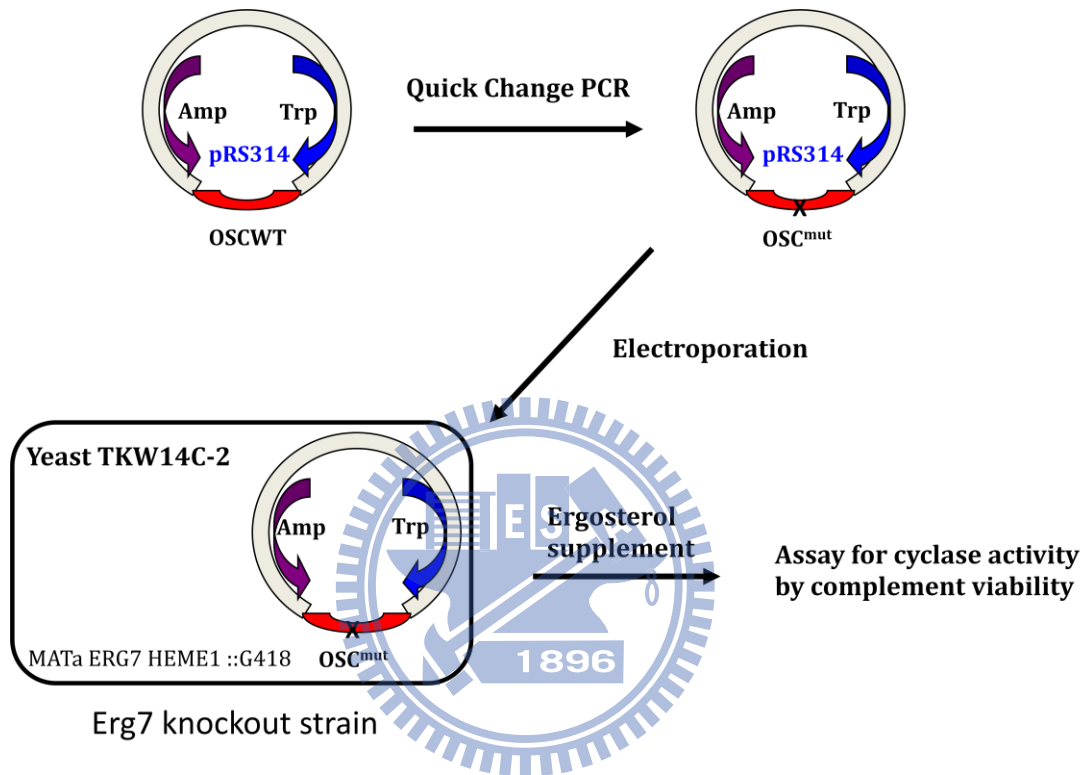


**Figure 3.1 The earlier stage analysis by ergosterol supplementation in TKW14C2 strains.**

**Table 3.1 The site-saturated mutants of *S.c* ERG7[C703X] and their genetic analysis.**

| *Sce*ERG7[703X] | | Restriction enzyme mapping | Sequence confirmation | Ergosterol supplement |
|---|---|---|---|---|
| Hydrophobic | Gly | | v | Live |
| | Ala | | v | Die |
| | Val | | v | Live |
| | Leu | | v | Die |
| | Ile | | v | Live |
| Aromatic | Phe | | v | Die |
| | Tyr | | v | Die |
| | Trp | | v | Die |
| Hydrophilic | Ser | | v | Live |
| | Thr | *Mfe* I | v | Live |
| Amidic | Asn | | v | Live |
| | Gln | | v | Die |
| Acidic | Asp | | v | Live |
| | Glu | | v | Die |
| Basic | His | | v | Live |
| | Lys | | v | Die |
| | Arg | | v | Die |
| other | Pro | | v | Die |
| | Met | | v | Die |

### 3.1.2 Product analysis

In order to analyze the function of C703 in the oxidosqualene cyclization and rearrangement cascade, the mutants were incubated in 2.5 L YNB culture for 2 weeks. After that, the saponification reaction was conducted, then the non-saponifiable lipid was extracted. Next, products were isolated by using silica gel column separation, then analyzing the structures of products by using gas chromatography-mass spectrometry **(Fig. 3.2)**.
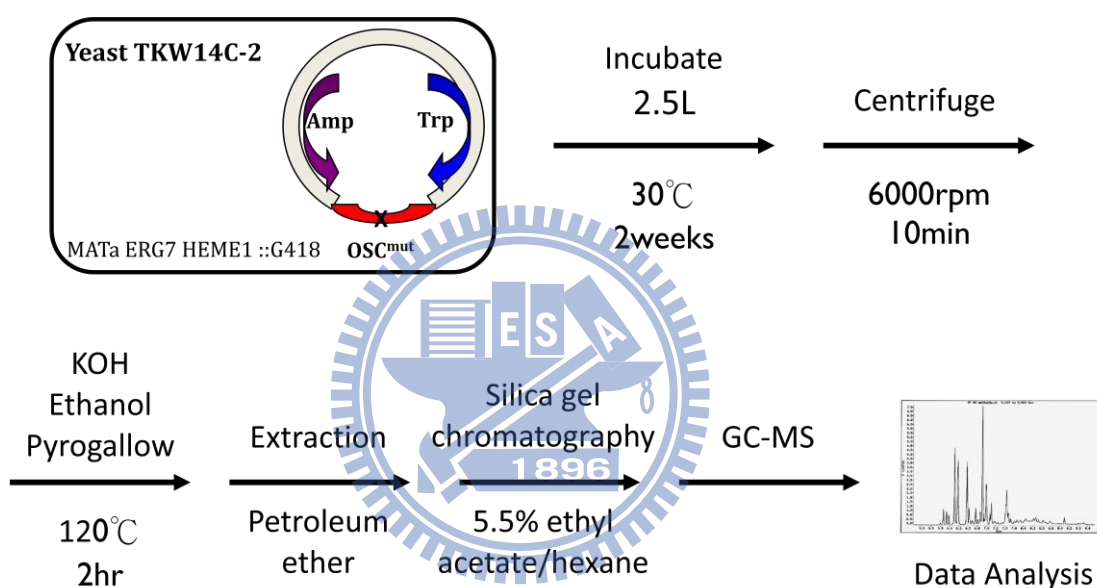


**Figure 3.2 Strategies of product purification and analysis.**

Cys703 is a second-sphere residue in the OSC active site, the Phe699 residue is between the substrate and Cys703. Therefore, the mutation of Cys703 will indirectly affect the C-17 cation intermediate stability by the residue Phe699, as a result, this leads to the product analysis result of Cys703 mutation similar to the previous study result of Phe699 **(Table 3.2)**.

# Table 3.2 The product analysis of *S. cerevisiae* ERG7 C703^mut

| C703X | Product pattern |
|---|---|
| N, D | LA |
| P, R | LA (minor) |
| Q, K | Protosta-13(17),24-dien-3β-ol (minor) |
| A, L, F, Y, W, E | No product |

| C703X | (13αH)-malabarica-14E,17E,21-trien-3β-ol | (13αH)-isomalabarica-14E,17E,21-trien-3β-ol | (13αH)-isomalabarica-14Z,17E,21-trien-3β-ol | (13αH)-isomalabarica-14(26),17,21-trien-3β-ol | Protosta-13(17),24-dien-3β-ol | Protosta-16,24-dien-3β-ol | Protosta-17(20),24-dien-3β-ol | Protosta-20,24-dien-3β-ol | 17α-Protosta-20,24-dien-3β-ol | 17α-protosta-20(22),24-dien-3β-ol | Lanosterol | unknown |
|---|---|---|---|---|---|---|---|---|---|---|---|---|
| I | 15 |  | 11 | 22 | 10 |  |  |  |  | 18 | 20 | 4 |
| M |  | 4 | 26 | 26 |  |  |  |  |  | 16 | 28 |  |
| H |  | 3 | 3 | 12 | 3 |  |  |  |  | 31 | 47 | 1 |
| S |  |  |  | 5 |  | 6 |  |  |  |  | 89 |  |
| V |  |  |  | 3 |  |  |  |  |  |  | 97 |  |
| T |  |  |  | 4 |  |  |  |  |  |  | 96 |  |
| G |  |  |  | 9 |  |  |  |  |  |  | 91 |  |

### 3.1.3 Proposed cyclization/rearrangement mechanism

The various products within ERG7[Cys703X] indicate that Cys703 is a crucial residue in the putative active site for catalytic function of lanosterol synthase. Nine products, including four truncated cyclization tricyclic structures and four tetracyclic structures and one unknown, are identified from various ERG7[C703X] mutants.

Four truncated tricyclic compounds include:

    i.    (13α*H*)-malabarica-14E,17E,21-trien-3β-ol

    ii.   (13α*H*)-isomalabarica-14E,17E,21-trien-3β-ol

    iii.  (13α*H*)-isomalabarica-14Z,17E,21-trien-3β-ol

    iv.  (13α*H*)-isomalabarica-14(26),17,21-trien-3β-ol.

These data suggest that after oxidosqualene pre-folds into chair-boat-chair conformation and then follows the cyclization step via cation-π interactions to a 6,6,5-tricyclic C-14 cation intermediate, these three (13α*H*)-isomalabarica-trien-3β-ols will derive from deprotonation at C-15 or C-26 of the 6,6,5-tricyclic C-14 cation. However, the mechanism of first compound (13α*H*)-malabarica-14E,17E,21-trien-3β-ol is not typical, it is pre-folded into chair-chair-chair conformation first, then performs the cyclization steps.

In addition, the anti-Markovnikov expansion of the five-membered C-ring to form 6,6,6-tricyclic C-13 cation, and then via normal D-ring closure generates protosteryl C-20 cation, some parts of substrates through a series of methyl and hydride shifts, deprotonation at C-8 or C-9 and yields lanosterol. In addition, the mutation of Cys703 may influence the Phe699 residue so that it affects the stability of the C-17 cation intermediate during or after the protosteryl cation formation, where it generates the truncated or different stereochemical triterpenes including:

    i.    Protosta-13(17),24-dien-3β-ol

    ii.   Protosta-16,24-dien-3β-ol

iii.    17α-protosta-20(22),24-dien-3β-ol

Different from the previous characterization, an amazing phenomenon occurs in the Cys703 mutation, the 17α-protosta-20(22),24-dien-3β-ol structure is observed in the Ile, Met, and His mutant **(Fig. 3.3)**. The speculated pathway is the unnatural D-ring closure, α-orientation of the large side-chain, and then the generation of the 17α-protosteryl C-20 cation. In the previous study, the near absence of 17α dammarenyl cyclases in higher plants reflects the rarity of the 17β to 17α evolutionary step. Therefore, disregarding protosteryl or dammarenyl cations, the 17α configuration is unusual and rare in the cyclization process. Formation of 17α-derivatives is un-natural, and the proposed pathway via 17α protosteryl C-20 cation could not be defined in the mechanism of the wild-type cyclases. On the other hand, the 17α configuration intermediates did appear only in bacteria or derived from rare plant species, indicating that the 17α configuration may exist in early evolutionary periods, which could rationally explain the rarity of the 17α-derivatives.
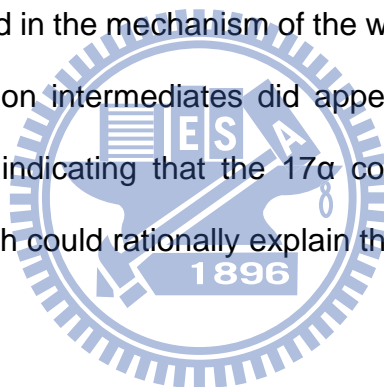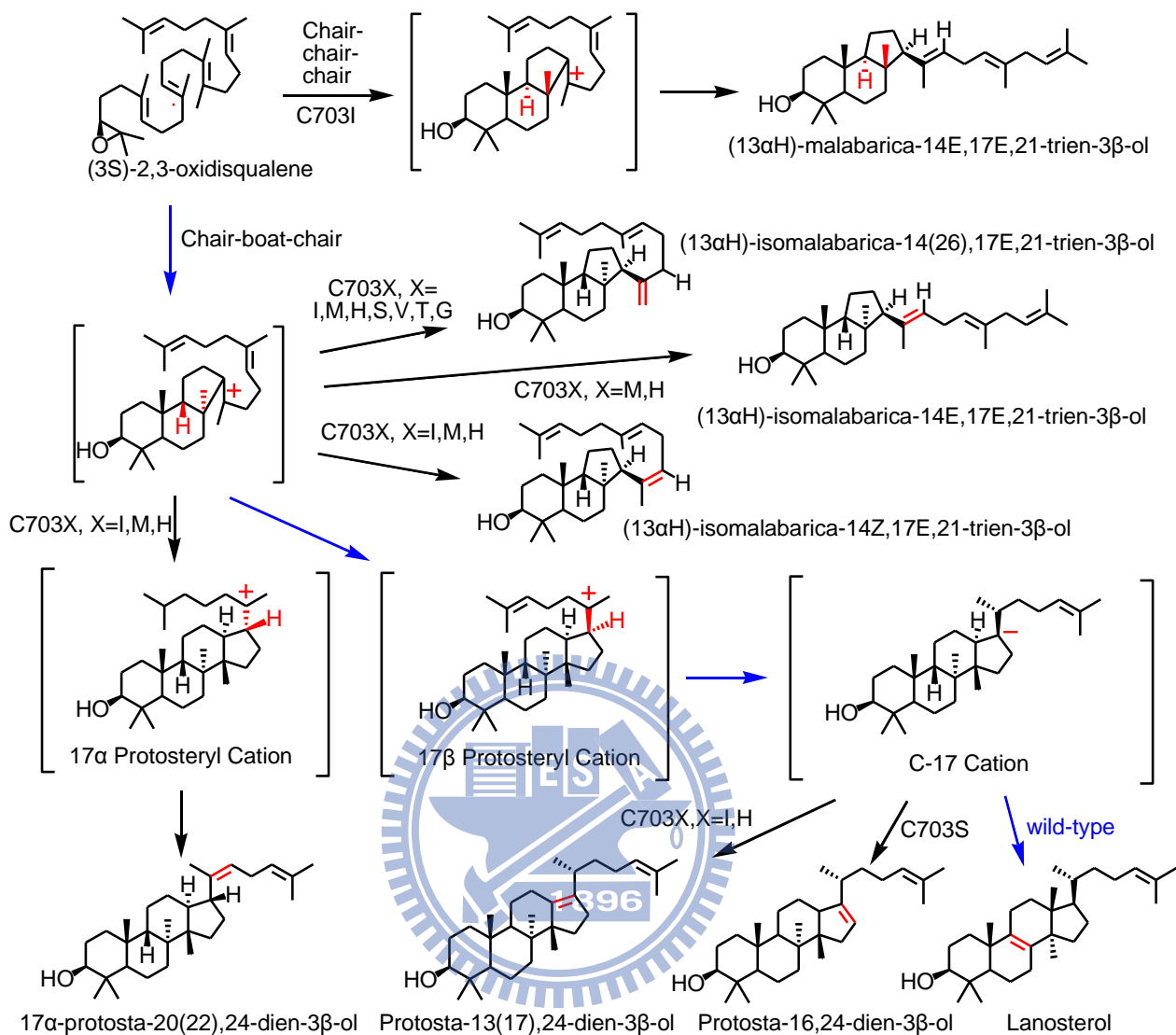
**Figure 3.3 Proposed cyclization/rearrangement pathway occurring in the ERG7^C703X site-saturated mutants.**

## 3.1.4 Analysis of the ERG7$^{C703X}$ mutants with homology modeling

Molecular modeling studies were performed to investigate the roles of important residues in the cyclization and rearrangement cascade. Due to the lack of a high-resolution crystal structure of *S. cerevisiae* ERG7, the homology models of *S. cerevisiae* ERG7 and its mutated ERG7 proteins were derived from the human OSC X-ray structure as the template, and it was complexed with lanosterol or 6,6,5-tricyclic C-14 cation or 17α-protosteryl cation, together with product profiles. In order to investigate the relationship between enzyme structure and product specificity, the homology model of ERG7 showed that Cys703 is a secondary residue in the activity site, and the residue Phe699 is between Cys703 and the substrate lanosterol **(Fig. 3.4)**.
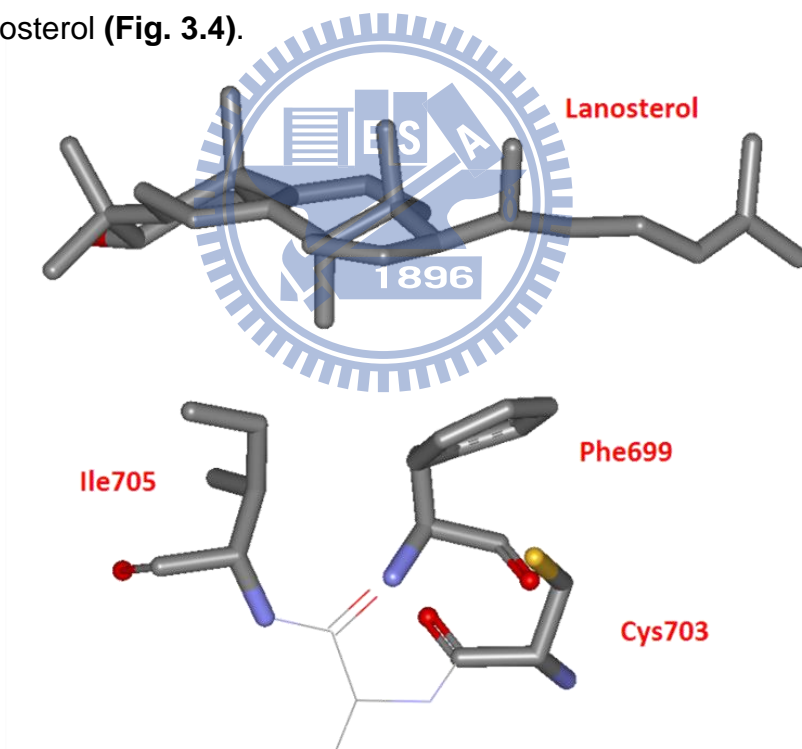


**Figure 3.4 Homology model of Cys703 complex with Phe699, Ile705 and lanosterol.**

The situation and property of Cys703 are considered to have some interaction with the Phe699, which and then can affect the substrate. According to the product profiles of Cys703X that contain the 6,6,5-tricyclic C-14 cation and 17α-protosteryl

cation which are similar to that of Phe699 mutations, further studies to determine the function of Cys703 for Phe699 will be carried out.

Steric effect is predicted to be a more reasonable phenomenon of the products distribution. The aromatic mutants Phe, Tyr and Trp have large functional groups that causing serious steric effect. In particular, these residues make a large gap between Phe104 and Leu145, where the distance increased between them is approximately from 3.8Å to 7.2Å **(Figure 3.5A)**. In addition, the effect by mutant Glu and Gln are similar to the effect by those aromatic residues, where their side chains also influence the Phe104 and Leu145, making a change in the enzyme structure. Moreover, when the mutants have longer linear residues like Arg and Lys, they almost lose their functions **(Figure 3.5B)**.
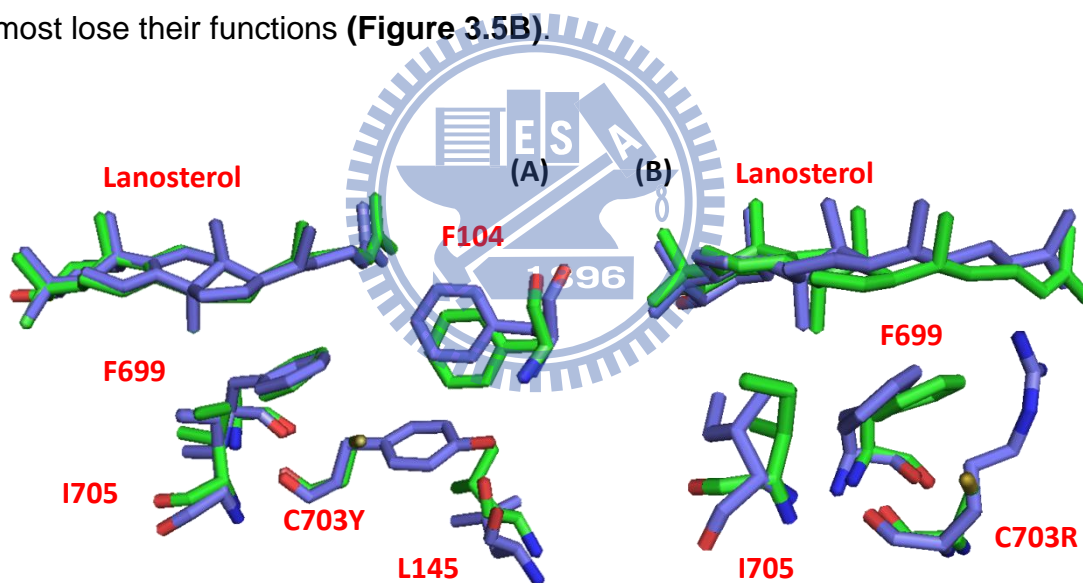


**Figure 3.5 Homology model of Cys703 mutant complex with Phe699, Ile705 and lanosterol. Green is the wild-type ERG7, and blue one is the mutant. (A) Cys703Tyr. (B) Cys703Arg.**

Although residues Cys703Ile, Cys703Met and Cys703His mutants change to a large group, they do not cause exaggerated steric effects. However, the oxidosqualene-lanosterol cyclase seems not to fold the substrate well, this effect introduces interruption of the last cyclization step, and generates truncated tricyclic triterpenoid products **(Fig. 3.6)**.
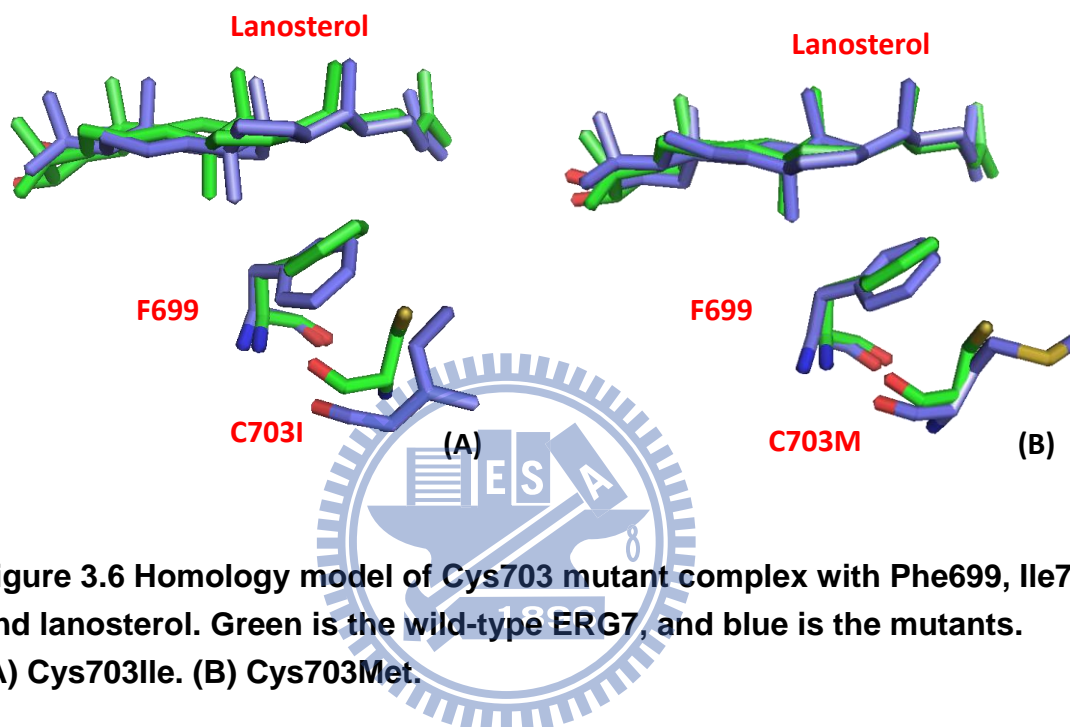


**Figure 3.6 Homology model of Cys703 mutant complex with Phe699, Ile705 and lanosterol. Green is the wild-type ERG7, and blue is the mutants. (A) Cys703Ile. (B) Cys703Met.**

In addition, production of the protosta-13(17),24-dien-3β-ol and the protosta-16,24-dien-3β-ol is due to the compression of the residue Phe699 by the mutated Cys703 residue, which generates an unstable C-17 cation and causes an earlier deprotonation step.

Furthermore, Cys703 mutations produced a 17α side chain product, 17α-protosta-20(22),24-dien-3β-ol. As shown in **Figure 3.7**, the left side is the wild-type pre-folding conformation, whereas the right side is the pre-folding conformation of the mutant. It reveals that the mutation changes the Phe699 position that leads to the region below C-17, which becomes flexible and results in the production of the 17α product.
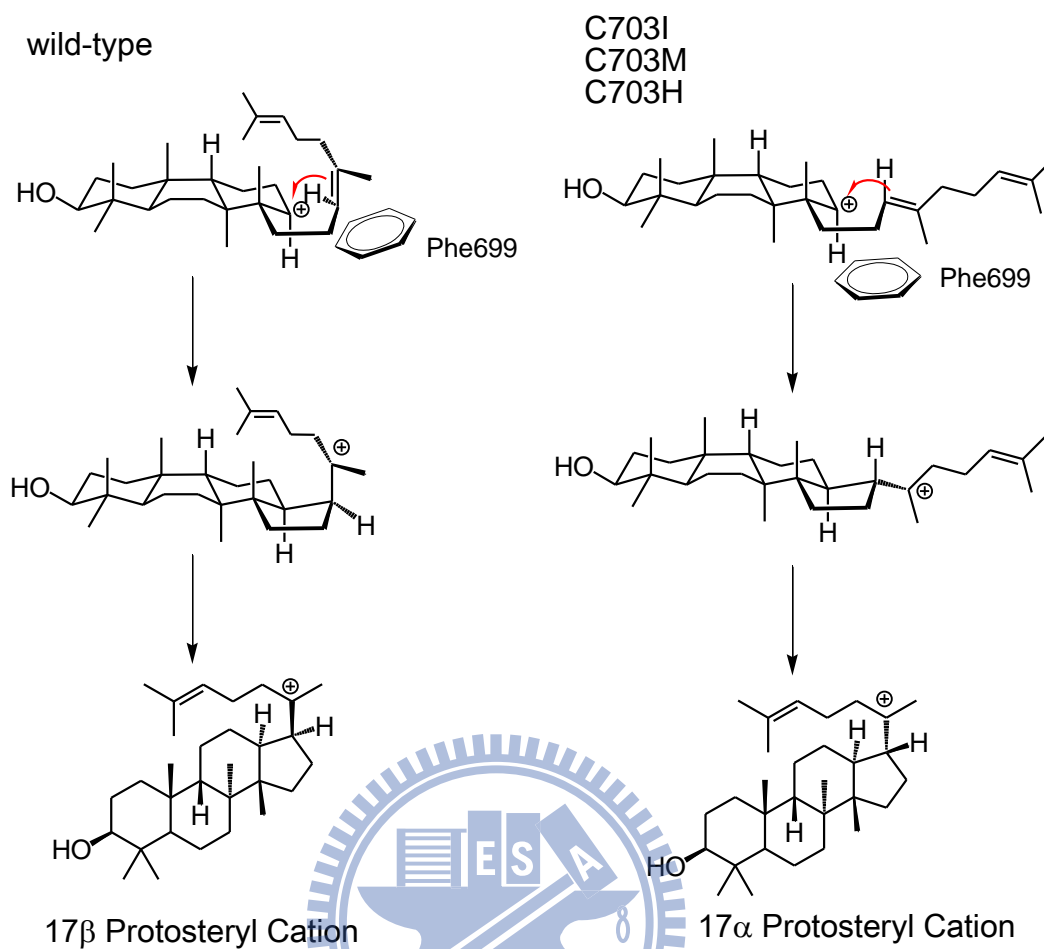
**Figure 3.7 Proposed mechanism of the production of the 17α product.**

Moreover, the amino acid Ile is well known for a large hydrophobic residue. As mentioned earlier, the change of residue Cys703 to Ile produces a 17α product. On the other hand, the mutant can even change the substrate pre-folding structure, converting the B-ring to chair conformation, and finally produce (13α*H*)-malabarica-14E,17E,21-trien-3β-ol.

According to these phenomena, it is proposed that the residue Cys703 has a strong relationship to nearby residues. The interaction between Cys703 and Phe699 might be a key point to understand the characteristics of Cys703. Hence, the double mutant of Cys703 and Phe699 was constructed, and the results are shown in the next section.

### 3.1.5 Product analysis of the double mutant of ERG7[F699X/C703I]

When comparing the products distribution of Cys703, Phe699 and Ile705, there are some interesting results.[43-44] From the entire product pattern, the Cys703 mutants produced more truncated tricyclic compounds while the Phe699 and I705 mutants produced more tetracyclic compounds. However, to focus on the 17α-orientation compounds, the 17α-protosta-20(22),24-dien-3β-ol was the major compound in the Cys703 and Ile705 mutants, while the Phe699 mutants have the 17α-protosta-20,24-dien-3β-ol product **(Table 3.3)**.

**Table 3.3 the product pattern of C703, F699 and I705 in *S. cerevisiae***

| ERG7^mut | (13αH)-malabarica-14E,17E,21-trien-3β-ol | (13αH)-isomalabarica-14E,17E,21-trien-3β-ol | (13αH)-isomalabarica-14Z,17E,21-trien-3β-ol | (13αH)-isomalabarica-14(26),17,21-trien-3β-ol | Protosta-13(17),24-dien-3β-ol | Protosta-16,24-dien-3β-ol | Protosta-17(20),24-dien-3β-ol | 17α-Protosta-20,24-dien-3β-ol | 17α-protosta-20(22),24-dien-3β-ol | Lanosterol | unknown |
|---|---|---|---|---|---|---|---|---|---|---|---|
| | Product pattern (%) | | | | | | | | | | |
| C703I | 15 | | 11 | 22 | 10 | | | | 18 | 20 | 4 |
| C703M | | 4 | 26 | 26 | | | | | 16 | 28 | |
| C703H | | 3 | 3 | 12 | 3 | | | | 31 | 47 | 1 |
| F699N | 6 | | | | 62 | | 12 | 20 | | | |
| F699H | | | | | 70 | | 17 | | | 13 | |
| F699K | | | | | 63 | | 17 | 20 | | | |
| F699T | | | | | 99 | | | | | 1 | |
| F699M | 7 | 17 | 18 | | 46 | | 10 | 1 | | 1 | |
| I705F | | | | 21 | | 6 | | 6 | 42 | 25 | |

According to the compound distribution, the characteristics of the Cys703 residue might proximity to Ile705 than Phe699. In a previous study[44], the Ile705, a second-sphere residue, was proposed to affect the substrate via influencing the Phe699 residue. In order to confirm the relationship between Phe699 and Cys703, the investigation of Phe699/Cys703 double mutation was required. Cys703 mutants produce various compounds that are similar to Phe699 mutants, but the compound 17α-protosta-20(22),24-dien-3β-ol only appears in Cys703 mutants. Therefore, the Cys703Ile was chosen to construct the double mutant, and their products analysis will be discussed later.

**Table 3.4 Product analysis of *S. cerevisiae* ERG7[F699X/C703I] double mutants**

| ERG7[mut] | (13αH)-malabarica-14E,17E,21-trien-3β-ol | (13αH)-isomalabarica-14E,17E,21-trien-3β-ol | (13αH)-isomalabarica-14Z,17E,21-trien-3β-ol | (13αH)-isomalabarica-14(26),17,21-trien-3β-ol | Protosta-13(17),24-dien-3β-ol | Protosta-16,24-dien-3β-ol | Protosta-17(20),24-dien-3β-ol | Protosta-20,24-dien-3β-ol | 17α-Protosta-20,24-dien-3β-ol | 17α-protosta-20(22),24-dien-3β-ol | Lanosterol | unknown |
|---|---|---|---|---|---|---|---|---|---|---|---|---|
| C703I | 15 | | 11 | 22 | 10 | | | | | 18 | 20 | 4 |
| F699A | No product | | | | | | | | | | | |
| F699A/C703I | No product | | | | | | | | | | | |
| F699M | 7 | 17 | 18 | | 46 | | 10 | | 1 | | 1 | |
| F699M/C703I | No product | | | | | | | | | | | |
| F699T | | | | | 99 | | | | | | 1 | |
| F699T/C703I | | | | | 67 | | 13 | | | 5 | 15 | |

In the experiment with Phe699Ala/Cys703Ile double mutants and Phe699Met/Cys703Ile double mutants, there were no products found **(Table 3.4)**. It is probable that the mutation in this area of enzyme active-site may change the enzyme conformation. Hence, these two double mutants lost the activity **(Figure 3.8)**.
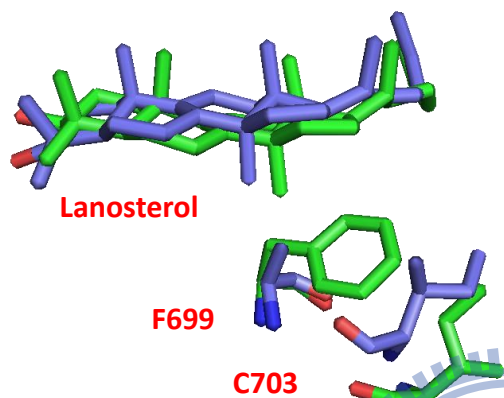


**Figure 3.8 Homology model of the double mutant complex with lanosterol. Green is the single mutation on Cys703, and blue is the F699A/C703I double mutants.**

Fortunately, interesting data were discovered in the Phe699Thr/Cys703Ile double mutation, except for the formation of a little amount of lanosterol, the single mutant of Phe699Thr produced protosta-13(17),24-dien-3β-ol as the major compound. The generation of protosta-13(17),24-dien-3β-ol and 17α-protosta-20,24-dien-3β-ol also appeared in the double mutant of Phe699Thr/Cys703Ile. The product distribution of the F699T/C703I double mutant is similar to the pattern of the F699T mutant instead of the pattern of C703I. This result showed that Cys703 is an important assistant residue to the first-sphere residue Phe699, which provides the correct position. An appropriate residue not only avoids the truncating reaction to produce a tricyclic compound, but also prevents the side-chain pre-folding toward to wrong angle, finally enabling the synthesis of the product accurately.

## 3.2 Functional analysis of CAS1 within *A. thaliana*

### 3.2.1 Site-directed alanine-scanning mutagenesis

In this section, the site-directed alanine-scanning mutagenesis was used. The focus was on the 15 residues in the activity site that are highly conserved in CAS1 from *Arabidopsis thaliana.* Besides constructing 15 different mutations generated by using QuikChange Site-Directed Mutagenesis kit, the mutated plasmids were evaluated by using a restriction enzyme mapping check. All mutated plasmids were confirmed by DNA sequencing using an ABI PRISM 3100 DNA sequencer.

The recombinant plasmids were transformed into TKW14C2 and the ergosterol supplementation was administered by same strategies as was described in **Section 3.1.1**. The result shows that it is necessary for exogenous ergosterol to grow since the plant CAS gene does not produce the lanosterol **(Table 3.5)**.

**Table 3.5 The genetic analysis of *A. thaliana* CAS^mut^.**

| *Ath*CAS1^mut^ | Restriction enzyme mapping | Sequence confirmation | Ergosterol supplement |
|---|---|---|---|
| V368A | *Sac* I | v | Die |
| L372A | *Sac* I | v | Die |
| W416A | *Sac* I | v | Die |
| F472A | *Sac* I | v | Die |
| C484A | *Not* I / *Xho* I | v | Die |
| E548A | *Sac* II | v | Die |
| F550A | *Sac* II | v | Die |
| I553A | *Sac* II | v | Die |
| W610A | *Kpn* I | v | Die |
| Y616A | *Kpn* I | v | Die |
| F726A | *Stu* I / *Xho* I | v | Die |
| C730A | *Stu* I / *Xho* I | v | Die |
| I732A | *Ssp* I | v | Die |
| Y734A | *Ssp* I | v | Die |
| Y737A | *Ssp* I | v | Die |

## 3.2.2 Product analysis

In this section, the products of these mutants are related to the abnormal products within *Sce*ERG7 **(Table 3.6)**.

**Table 3.6 The product analysis of *A. thaliana* CAS[mut].**

| CAS1[mut] | (9R,10S)-polypoda-8(26),13E,17E,21-tetraen-3β-ol | (13αH)-isomalabarica-14(26),17,21-trien-3β-ol | Protosta-13(17),24-dien-3β-ol | Protosta-17(20),24-dien-3β-ol | Lanosterol | Parkeol | Cycloartenol |
|---|---|---|---|---|---|---|---|
| V368A | | | | | | 1 | 99 |
| L372A | No product | | | | | | |
| W416A | No product | | | | | | |
| F472A | | 36 | | | 22 | 8 | 34 |
| C484A | | | | | 2 | 3 | 95 |
| E548A | | | | | | 1 | 99 |
| F550A | | | | | | 2 | 98 |
| I553A | No product | | | | | | |
| W610A | No product | | | | | | |
| Y616A | | | | | | 4 | 96 |
| F726A | | | 22 | 14 | | 29 | 35 |
| C730A | | | | | | 2 | 98 |
| I732A | | | | | | | 100 |
| Y734A | 5 | | | | 39 | 9 | 47 |
| Y737A | | | | | 3 | 2 | 95 |

### 3.2.3 Proposed cyclization/rearrangement mechanism

The cycloartenol was produced by the wild-type cycloartenol synthase. The bicyclic compound, (9R,10S)-polypoda-8(26),13E,17E,21-tetraen-3β-ol, was produced by the Tyr734Ala mutant. In addition, the Phe472Ala mutant produces a tricyclic compound (13αH)-isomalabarica-14(26),17,21-trien-3β-ol. Moreover, Protosta-13(17),24-dien-3β-ol and Protosta-17(20),24-dien-3β-ol, two tetracyclic products, were found in the Phe728Ala mutant **(Figure 3.9)**.
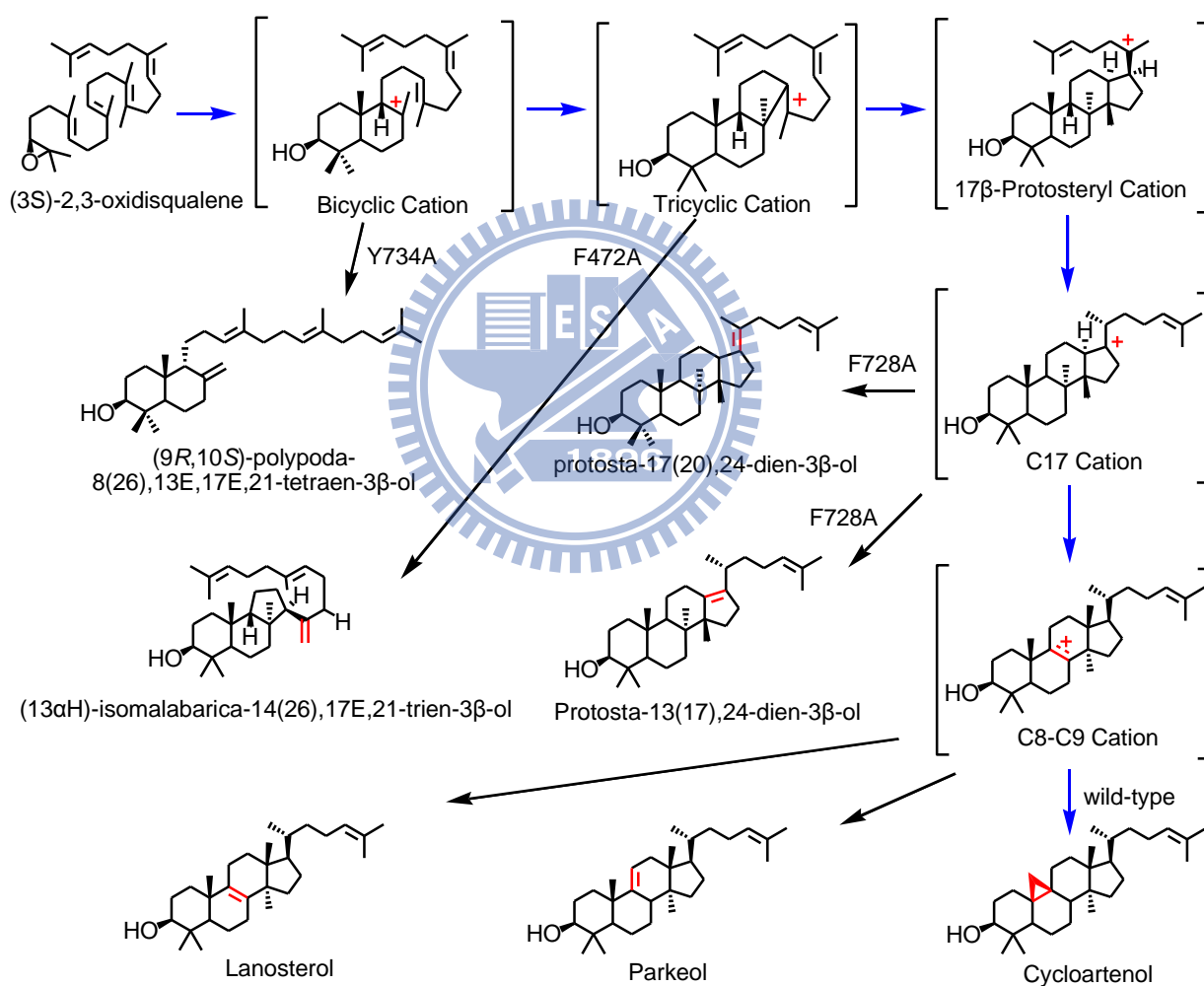


**Figure 3.9 Proposed cyclization/rearrangement pathway occurring in CAS1[mut]**

When focusing on comparing the products distribution of CAS1 and ERG7, there are some interesting points to observe **(Table 3.7)**.[45-47]

**Table 3.7 The product analysis of *Ath*CAS mutants comparing to the corresponding residue mutants in *Sce*ERG7**

| | Product Pattern (%) | | | | | | | |
|---|---|---|---|---|---|---|---|---|
| | (9R,10S)-polypoda-8(26),13E,17E,21-tetraen-3β-ol | (13αH)-isomalabarica-14(26),17,21-trien-3β-ol | Protosta-13(17),24-dien-3β-ol | Protosta-17(20),24-dien-3β-ol | Lanosterol | Parkeol | Cycloartenol | 9β-lanosta-7,24-dien-3β-ol |
| CAS1[F472A] | | 36 | | | 22 | 8 | 34 | |
| ERG7[F445T] | | 49 | | | 46 | | | 5 |
| CAS1[F726A] | | | 22 | 14 | | 29 | 35 | |
| ERG7[F699H] | | | 70 | 17 | 13 | | | |
| CAS1[Y734A] | 5 | | | | 39 | 9 | 47 | |
| ERG7[Y707H] | 84 | | | | 5 | 5 | | 6 |

First, (13αH)-isomalabarica-14(26),17,21-trien-3β-ol is produced from the *Ath*CAS1 Phe472 mutant. It is a tricyclic compound and is found in His234 and Phe445 mutants in *Sce*ERG7, SceERG7[Phe445] and is corresponding to CAS1[Phe472]. Even though His234 and Phe445 are located in different situations, both of them were discovered to influence C-ring cyclization reactions.[45]
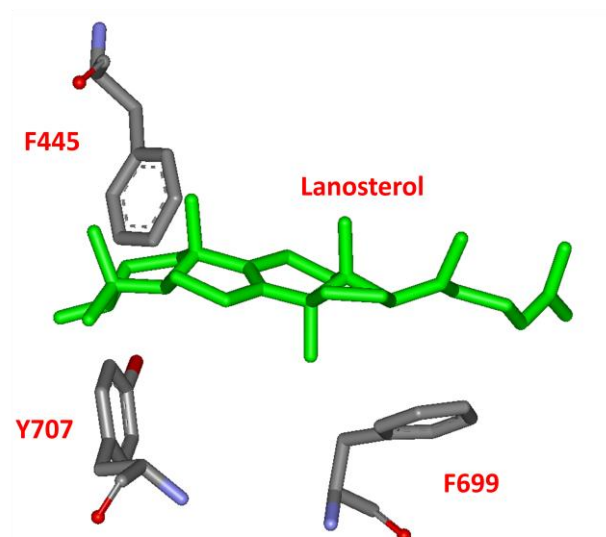
**Figure 3.10 Homology model of F445, F699 and Y707 in *Sce*ERG7 mutant complex with lanosterol.**

The mutation of Phe726 to Ala produces two abnormal products, protosta-13(17),24-dien-3β-ol and protosta-17(20),24-dien-3β-ol instead of lanosterol. They are tetracyclic compounds which can be found in *Sce*ERG7 Phe699, and that corresponds to *Ath*CAS1 Phe726. In addition, *Sce*ERG7[Phe699] is well known for stablizing the C-17 cation.[46]

Lastly, (9*R*,10*S*)-polypoda-8(26),13E,17E,21-tetraen-3β-ol is a bicyclic compound made by Tyr734Ala. This compound is also found in the *Sce*ERG7 Tyr707 mutant which corresponds to *Ath*CAS1 Tyr734. In the previous study[47], *Sce*ERG7 Tyr707 is predicted to stabilize the C-8 cation in the cyclization step. Mutation of this residue to a small, non-aromatic residue, causes the cation to be unstable, and subsequently stops the C-ring cyclization.

## 3.3 Functional analysis of *P. sativum* PSY

### 3.3.1 Site-directed alanine-scanning mutagenesis

Identical to section 3.2, 15 different mutations in *Pisum sativum* PSY were constructed by using QuikChange Site-Directed Mutagenesis kit. The mutated plasmids were evaluated by using a restriction enzyme mapping check. All mutated plasmids were confirmed by DNA sequencing using the ABI PRISM 3100 DNA sequencer.

The recombinant plasmids were transformed into TKW14C2 and the ergosterol supplementation was performed by the same strategies described in **Section 3.1.1**. The results show that the exogenous ergosterol is necessary for growth because the plant PSY gene does not produce the lanosterol **(Table 3.8)**.

**Table 3.8 The genetic analysis of *P. sativum* PSY<sup>mut</sup>.**

| PSY<sup>mut</sup> | Restriction enzyme mapping | Sequence confirmation | Ergosterol supplement |
|---|---|---|---|
| V371A | *Mfe* I | v | Die |
| L374A | *Stu* I / *Xho* I | v | Die |
| W418A | *Hind* III | v | Die |
| F474A | *Nco* I / *Xho* I | v | Die |
| C486A | *Nco* I / *Xho* I | v | Die |
| E550A | *Bgl* I | v | Die |
| F552A | *EcoR* I / *Xho* I | v | Die |
| I555A | *EcoR* I / *Xho* I | v | Die |
| W612A | *Nae* I | v | Die |
| Y618A | *Pvu* II | v | Die |
| F728A | *BspH* I | v | Die |
| C732A | *BspH* I | v | Die |
| I734A | *Nru* I / *Nde* I | v | Die |
| Y736A | *Nru* I / *Nde* I | v | Die |
| Y739A | *Nru* I / *Nde* I | v | Die |

## 3.3.2　Experimental results and phenomena

There are nine mutants that have the ability to produce β-amyrin including Leu374Ala, Phe728Ala, Tyr739Ala mutants which have reduced β-amyrin production **(Table 3.9)**. The residue Phe552Ala is the only mutant that produces lupeol from alanine scanning in our laboratory. The production of lupeol suggests that after oxidosqualene cyclized to the lupenyl cation intermediate, the cation intermediate is unstable in PSY^Phe552Ala and the E-ring expansion will not occur, finally producing lupeol.

**Table 3.9 The product analysis of *P. sativum* PSY^mut.**

| PSY^mut | Product pattern (%) | |
|---|---|---|
| | β-amyrin | Lupeol |
| V371A | 100 | |
| L374A | (minor) | |
| W418A | No product | |
| F474A | No product | |
| C486A | 100 | |
| E550A | 100 | |
| F552A | 73.3 | 26.7 |
| I555A | No product | |
| W612A | No product | |
| Y618A | 100 | |
| F728A | (minor) | |
| C732A | 100 | |
| L734A | No product | |
| Y736A | No product | |
| Y739A | (minor) | |
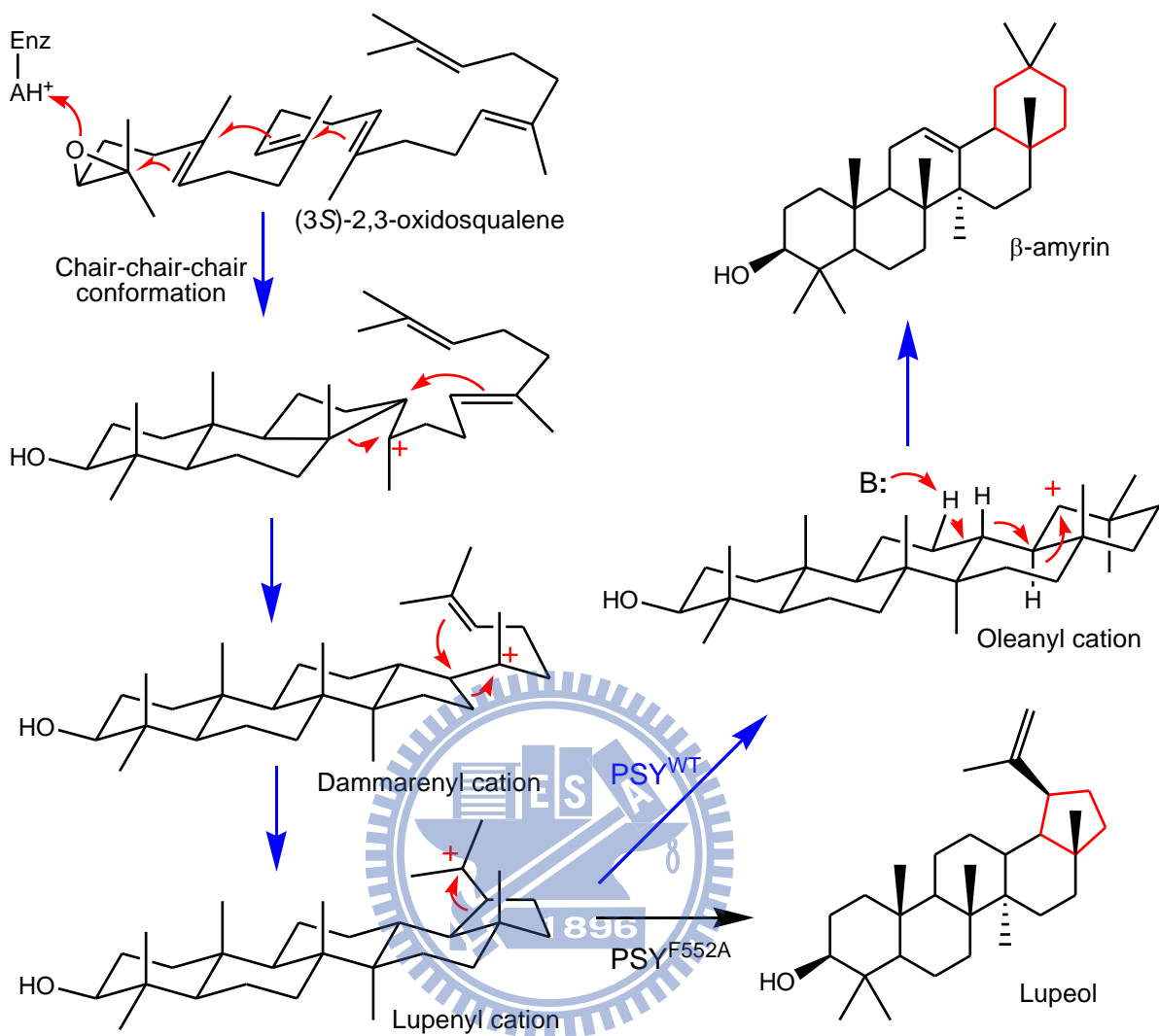
**Figure 3.11 Proposed cyclization/rearrangement pathway occurring in PSY$^{mut}$**

From the homology modeling, the position of this residue is near to the tail of the substrate in the enzyme active-site. The second sphere residue, the F552A mutant, might interact with its neighboring residues to influence the E-ring expansion step **(Fig. 3.12)**. To study the site-saturated mutagenesis on Phe552 or Met729 further should give more detailed information to propose more convictive mechanism on the last cyclization step.
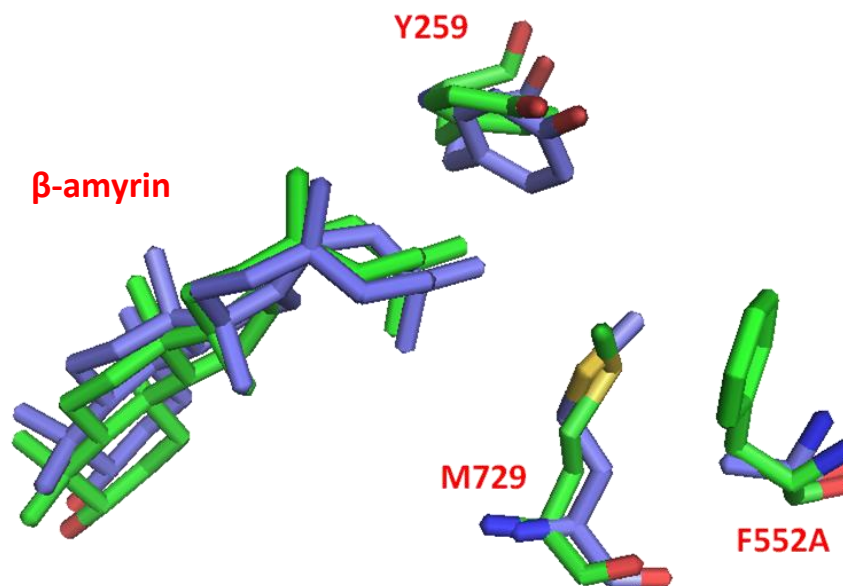
**Figure 3.12 Phe552, Tyr259 and Met729 complex with β-amyrin.**

The mutants Trp418Ala, Phe474Ala, Ile555Ala, Trp612Ala, Ile734A and Tyr736Ala, all lose the activity of enzyme function. Although the mutations cause a large major changing of the residue size which could destroy the whole enzyme structure, there is something additional worth noting. While comparing the product pattern of PSY with the CAS1 pattern, it shows that there are some similarities and dissimilarities. The mutation points which cause loss of the enzyme activity are similar except for the last three residues **(Table 3.10)**. Thus, the mutations of these three residues do not seem to cause any structural change different from the proposed modeling. These data indicate that these residues play a different role between PSY and CAS1. These residues may be important to B-chair ring formations **(Fig. 3.13)**. The position of these residues in PSY can be found in **Figure 1.20**. Based on this conclusion, it might be worthwhile to carry out further research in this area in the future.

**Table 3.10 Comparison of the product quantity between PSY and CAS1.**
**＋ means similar to wild-type, △ means reduced production,**
**— means no product.**

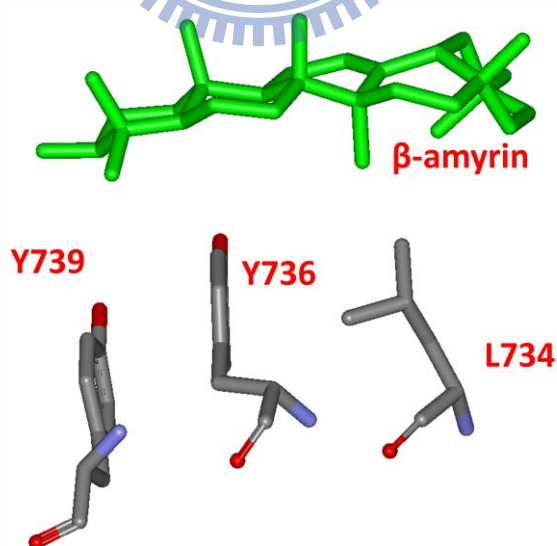| PSY^mut/CAS1^mut | PSY | CAS1 |
|---|---|---|
| V371A/V368A | ＋ | ＋ |
| L374A/L372A | △ | — |
| W418A/W416A | — | — |
| F474A/F472A | — | △ |
| C486A/C484A | ＋ | ＋ |
| E550A/E548A | ＋ | ＋ |
| F552A/F550A | △ | ＋ |
| I555A/I553A | — | — |
| W612A/W610A | — | — |
| Y618A/Y616A | ＋ | ＋ |
| F728A/F726A | △ | △ |
| C732A/C730A | ＋ | ＋ |
| L734A/I732A | — | ＋ |
| Y736A/Y734A | — | △ |
| Y739A/Y737A | △ | ＋ |



**Figure 3.13 Homology model of L734, Y736 and Y739 in PSY complex with β-amyrin.**

# Chapter 4   Conclusions

Site-directed mutagenesis is a useful molecular biology technique on the studies of enzymes. The relationship of structure-function-mechanisms of specific residues within putative active sites could be understood in depth using site-directed mutagenesis. The chemical compounds produced by mutated residues could provide clues on the functional roles in the cyclization and rearrangement reactions.

In this research, three oxidosqualene cyclases had been chosen for detailed analyses, including lanosterol cyclase within *Saccharomyces cerevisiae*, cycloartenol cyclase within *Arabidopsis thaliana* and β-amyrin synthase within *Pisum sativum*. The methods chosen were constructed for site-saturated mutagenesis or site-directed alanine-scanning mutagenesis. The experimental results indicate that the residues chosen for analysis are crucial within their cyclases. Herein are summarized several important conclusions in this research.

## 4.1   Analysis of *S. cerevisiae* ERG7$^{C703X}$ mutations

(1)   Construction of saturated mutants of ERG7$^{C703X}$ from *Saccharomyces cerevisiae* and the results of genetic analysis showed that half of the C703X mutations could complement ergosterol-deficient growth including Gly, Val, Ile, Ser, Thr, Asp, Asn and His.

(2)   Nine products were generated in ERG7$^{C703X}$ mutations with a molecular mass of       $m/z = 426$, including:

    i.    unknown

    ii.    (13α*H*)-malabarica-14E,17E,21-trien-3β-ol

    iii.    (13α*H*)-isomalabarica-14E,17E,21-trien-3β-ol

iv.    (13α*H*)-isomalabarica-14Z,17E,21-trien-3β-ol

v.    (13α*H*)-isomalabarica-14(26),17,21-trien-3β-ol.

vi.    Protosta-13(17),24-dien-3β-ol

vii.    Protosta-16,24-dien-3β-ol

viii.    17α-protosta-20(22),24-dien-3β-ol

ix.    Lanosterol

(3)    The similar products profile indicated C703 has a strong relationship with the F699 residue. C703 certainly affects the first-sphere residue F699 within putative active site of oxidosqualene-lanosterol cyclase.

(4)    The unnatural 17α-derivatives, 17α-protosta-20(22),24-dien-3β-ol, were generated not only in the C703, but also for F699 and I705. It provides more evidence that the neighboring residues will affect each other to control the function of an enzyme.

(5)    The product distribution of the F699T/C703I double mutant is similar to the pattern of the F699T mutant, rather than the pattern of C703I. It shows that the C703 residue is an important assistant residue to the first-sphere residue Phe699.

## 4.2    Analysis of *A. thaliana* CAS1 mutations

(1)    Construction of alanine-scanning mutants of CAS1 from *Arabidopsis thaliana* and the results of genetic analysis showed that there were no mutants that could grow without ergosterol, meaning all of them could not produce sufficient lanosterol.

(2)    There are three mutants that produce the same compound to their corresponding residues in lanosterol synthase. Including:

i. Y734A produced (9*R*,10*S*)-polypoda-8(26),13E,17E,21-tetraen-3β-ol that was found in the Y707 mutant within *Sce*ERG7.

ii. F472A produced (13α*H*)-isomalabarica-14(26),17,21-trien-3β-ol that was found in the F445 mutants within *Sce*ERG7.

iii. F726A produced protosta-13(17),24-dien-3β-ol and protosta-17(20),24-dien-3β-ol found in the F699 mutant within *Sce*ERG7.

The data demonstrate that even in different species, the active-site conformations were similar in those divergent enzymes.

(3) The enzyme function in L372A, W416A, I553A, W610A mutants was lost, where can propose that were some serious changes in enzyme conformation.

## 4.3　Analysis of *P. sativum* βAS mutations

(1) Construction of saturated mutants of PSY from *Pisum sativum* and the results of genetic analysis showed that there was no mutant growth without ergosterol, indicates tha none of them could produce lanosterol.

(2) The residue Phe552Ala must strongly relate to the E-ring formation and rearrangement step because it produced lupeol.

(3) The function of Trp418Ala, Phe474Ala, Ile555Ala, Trp612Ala mutants was lost, where we can propose that were some serious changes in enzyme conformation.

(4) Because the function of Ile734Ala and Tyr736Ala mutants was lost, there might be some relationship to B-chair ring formation.

# Chapter 5　Future prospects

It is remarkable that the replacement of conserved Cys703 of ERG7 with mutated residue generated such a diversity of products. Experimental results show that ERG7$^{C703}$ will indirectly influence the terminal cyclization and stereochemistry; specifically switch the stereochemistry of 17β into 17α orientation, and promote the new evolution of enzymatic functions. New organic methods using analogues or isotope could be designed to elucidate the detailed mechanism via the 17α-protosteryl cation intermediate. Combining many oxidosqualene cyclases such as β-amyrin synthase and cycloartenol synthase, should be examined to analyze their functional role in depth. A construct of a chimeric oxidosqualene cyclase can be done in the future, mixing the functions of multiple cyclases. Moreover, the control of chair-boat-chair and chair-chair-chair substrate pre-folding conformations by cyclases also unsolved and is worthy to pursue as a future direction of research.

In order to understand more detailed information on the catalytic functions of cyclases, the construction of *erg1 erg7 erg11* triple knockout mutant in yeast system could be developed for *in vivo* experiments via the addition of the substrate. This method could prevent the interference due to the downstream enzymes. Furthermore, the purification of yeast lanosterol synthase is also an important task for the future, where the resolution of yeast lanosterol synthase crystal structures will provide more information about the complex cyclization and rearrangement cascade.

# Appendix

## A.1    Enhance the protein expression by change the vectors

Because the proteins of oxidosqualene cyclase family are very difficult to purify, the improvement of materials and methods are needed. A major target is to improve and enhance the specific protein expression. The vectors that carry the oxidosqualene cyclases gene belong to pRS310 series in our lab. The pRS310 series are centromere plasmids, and they also are shuttle vectors that they can travel between *E. coli* and *S. cerevisae*[48].

The vector pRS420 series were derived from the pRS300 series, and they are also shuttle vectors[49]. Different from pRS310 series, the pRS300 and pRS420 series are chromosome-integrating plasmids. Employing the pRS420 series plasmids to substitute the old pRS310 series will enhance the protein expression level.

### A.1.1.  Construction of the plasmids

In order to construct new plasmids, the first thing required is to obtain the protein gene. A site of mutation has to be designed and a restriction site must be integrated, where the restriction enzyme will be used. In our lab, the *Ath*CAS1 is in vector pRS313, the *Sce*ERG7 and *Psa*PSY is in vector pRS314, so a different mutation was needed, respectively.

The pRS314 with *Sce*ERG7 and *Psa*PSY use the primers below to construct a KpnI restriction site at the start of the gene promoter, and then use KpnI and XhoI to obtain the actual gene.

**YCC-RS313_RS314-promoter-KpnI-1**

5'- CgC ggT ggC ggT ACC gAg CTA CgT C -3'

**YCC-RS313_RS314-promoter-KpnI-2**

5'- gAC gTA gCT Cgg TAC CgC CAC CgC g -3'

The pRS313 with *Ath*CAS1 uses the primers below to construct a *Xho*I restriction site at the start of the gene promoter, then uses *Xho*I and *Sal*I to obtain the gene.
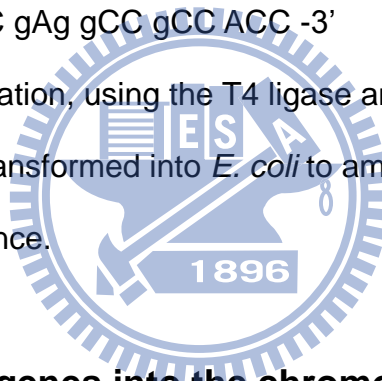
**YCC-RS313-promoter-XhoI-1**

5'- ggT ggC ggC CTC gAg CTA CgT CAg -3'

**YCC-RS313-promoter-XhoI-2**

5'- CTg ACg Tag CTC gAg gCC gCC ACC -3'

The next step was ligation, using the T4 ligase and reacting in 16°C overnight, then the plasmids were transformed into *E. coli* to amplify them. The plasmids were sent to confirm the sequence.

## A.1.2. Integrate the genes into the chromosome of TKW14C2

In this experiment, the Lithium acetate method was used. This method was based on the Gietz protocol with some modifications[50]. A 50 ml aliquot of ALTHMU medium was used to culture the TKW14C2, until $OD_{600}$=0.2 with 1:10 dilution, then centrifuged with 3000 x g, for 5min. The supernatant was discarded and the cells were resuspended in 4mL $ddH_2O$ and transferred to 4 eppendorf tubes, each containing 1 ml. The cell suspension was centrifuged for 1 min and the supernatant was discarded. The cell pellet was resuspended in 450 µl $ddH_2O$ and 50 µl 0.1 M LiAc and incubated for 10 min at 30 °C. The cell suspension was centrifuged for 1 min and the supernatant discarded. The transformation reagents were added to the cell pellet in the following order: 1 ml 50% PEG, 150 µl 1M LiAc, 5 µl 10 mg/ml

carrier ssDNA (preboiled for 5 min and cooled on ice), 3 μg linear plasmid DNA, ddH$_2$0 to total of 1.5 ml. The mix was vortexed to get a homogeneous suspension and incubated at 30°C for 30 min. The suspension was then heat-shocked at 42 °C for 20 min, then it was centrifuged for 1 min, and the supernatant was thoroughly removed. To the cell pellet 1 mL ddH$_2$0 was added, incubated at room temperature for 5 min and then resuspended by pipetting up and down, and gentle vortexing. The suspension was centrifuged for 1 min and the supernatant was discarded. The cells were resuspended in 200 μL ddH$_2$0 and plated on selective plates. Plates were incubated at 30°C until colonies were observed.

## A.1.3. Results and Discussion

The colony was selected and placed into 50 μl 0.02 M NaOH and boiled for 10 min, and then used the following composition and program was employed to do the genomic PCR to check that the gene was integrated into chromosome correctly **(Table A.1 & Table A.2)**.

**Table A.1 genomic PCR composition**

| Reagent | Volume (μl) | Total |
|---|---|---|
| Primer1 (1000 ng/μl) | 0.3 | |
| Primer2 (1000 ng/μl) | 0.3 | |
| Template | 4 | |
| dNTP (10 mM) | 0.4 | 20 |
| *Pfu* II buffer | 2 | |
| *Pfu* II polymerase | 0.2 | |
| DDW | 12.8 | |

**Table A.2 genomic PCR program**

| Segment | Cycles | Temperature (°C) | Time |
|---------|--------|------------------|------|
| 1 | 1 | 95 | 2 min |
| 2 | 35 | 95 | 1 min |
| | | 49 | 1 min |
| | | 68 | 3 min |
| 3 | 1 | 68 | 7 min |
| | | 4 | ∞ |

The same colony was also picked to do the product analysis. When the culture grew, the cells were harvested by centrifugation at 6000 rpm for 10 min, and 0.2 mg cholesterol was added per 1 g pellet as internal control. Then, by following the steps outlined in chapter 3, the analysis of the product pattern was constructed.

The results showed that the gene was cloned into the yeast strain correctly, but the efficiency of the expressed level was not better than the old method. It is possible that the transformant quality by the Lithium acetate method is not appropriate, and the property of internal control, cholesterol, is similar to ergosterol, which may cause problems in purification steps.

## A.1.4. Future work

The conditions of the Lithium acetate method, the selection of internal controls and the purification steps require improvement or new methods need to be derived that are more appropriate for the study material. After the issues as described above are resolved, and a more robust protein expression level is achieved, there will be many opportunities for further research in this exciting field. For example, *in vivo* experiments should be attempted. Through *in vivo* experiments, much information can be obtained about the enzyme activity of oxidosqualene cyclase, and then the research in this topic can achieve new insights into these important reactions.

## A.2     Construct *erg7/erg11* double knockout strain

In *Saccharomyces cerevisiae*, after the production of lanosterol within *erg7*, the downstream enzymes would consume the lanosterol to the other compounds. In order to avoid the interference of the compound distribution in the final product pattern, blocking the follow-up pathway is necessary. Therefore, because the products were accumulated, the analysis of the products would be more precise.

### A.2.1.  The sterol metabolic pathway within *S. cerevisiae*

The entire metabolic pathway begginning from farnesyl-pyrophosphate to ergosterol is shown in **Figure A.1**. The reaction started from two farnesyl-pyrophosphate **(1)**, then produce squalene **(2)** by squalene synthase within *erg9*. Next, through squalene epoxidase *erg1*, squalene becomes oxidosqualene **(3)**. Then, oxidosqualene converts into lanosterol **(4)** by oxidosqualene-lanosterol synthase *erg7*. In *Saccharomyces cerevisiae*, lanosterol changes into 4,4-dimethyl-ergosta-8,14,21-trienol **(5)** by C-14 demethylase *erg11*. Then, it becomes 4,4-dimethyl zymosterol (4,4-dimethylcholesta-8,24-dienol) **(6)** by $\Delta^{14}$-reductase *erg24*. After that, through C-4 sterol methyloxidase *erg25*, C-4 sterol decarboxylase *erg26* and C-3 sterol ketoreductase *erg27* to remove a methyl at C-4 situation, and produces 4-methyl zymosterol (4-methylcholesta-8,24-dienol) **(7)**. Repeat this step again producing zymosterol **(8)**. Next, zymosterol converts into fecosterol **(9)** by C-24 methyltransferse *erg6*. Then, fecosterol becomes episterol (cholesta-7,24(28)-dienol) **(10)** by $\Delta^8$-$\Delta^7$-reductase *erg2*. Though the C-5 desaturase *erg3*, ergosta-5,7,24(28)-trienol **(11)** is produced. And then, $\Delta^{22}$-desaturase *erg5* adds a double bond to ergosta-5,7,24(28)-trienol, producing ergosta-5,7,22,24(28)-tetraenol **(12).** Finally, ergosterol **(13)** is produced by the last

enzyme, $\Delta^{24(28)}$-reductase *erg4*. In addition, in different fungi species, the order of these reactions may be different[51-52]. Lanosterol can go through *erg6* to form 24-methylene lanosterol **(14)** first, and then converts to 4,4-dimethyl fecosterol **(17)** by *erg11* and *erg24*. Then, 4,4-dimethyl fecosterol can turn into 4-methyl fecosterol **(18)** by *erg25*, *erg26* and *erg27*. If this step is repeated again, it will form fecosterol **(9)**, and comes back to the normal pathway in *S. cerevisae*.

## A.2.2. The non-specificity of sterol metabolic enzymes

Different from most enzymes, the enzymes in the sterol metabolic pathway have less specificity. In other words, the enzymes will uptake the substrate, only if the substrate has a tetracyclic sterol skeleton. For example[53], in the *erg6* knockout strain, zymosterol would go through *erg2* to form cholesta-7,24-dienol **(19)**. If the *erg3* is still has function, the product will become cholesta-5,7,24-trienol **(20)** and cholesta-5,7,22,24-tetraenol **(21)**. Moreover, the *erg2* knockout strain will produce ergosta-8-enol **(22)**, ergosta-5,8-dienol and ergosta-5,8,22-trienol **(23)**, knockout *erg3* gene causing the production of ergosta-7-enol **(24)** and ergosta-7,22-enol **(25)**.

In previous studies[54-55], when *erg11* had been knocked out, the lanosterol could not remove the C-14 methyl group to form 4,4-dimethyl-ergosta-8,14,21-trienol, but the whole reaction would not be stopped. Instead, lanosterol would go through *erg6* to form 24-methylene lanosterol **(14)**, and then convert to 14-methyl fecosterol **(15)** by *erg25*, *erg26* and *erg27*. Unfortunately, if the *erg3* gene has not been knocked out this time, the 14-methyl fecosterol will be transformed into 14α-methylergosta-8,24(28)-dien-3β,6α-diol **(16)**, a toxic compound to *S. cerevisiae*.
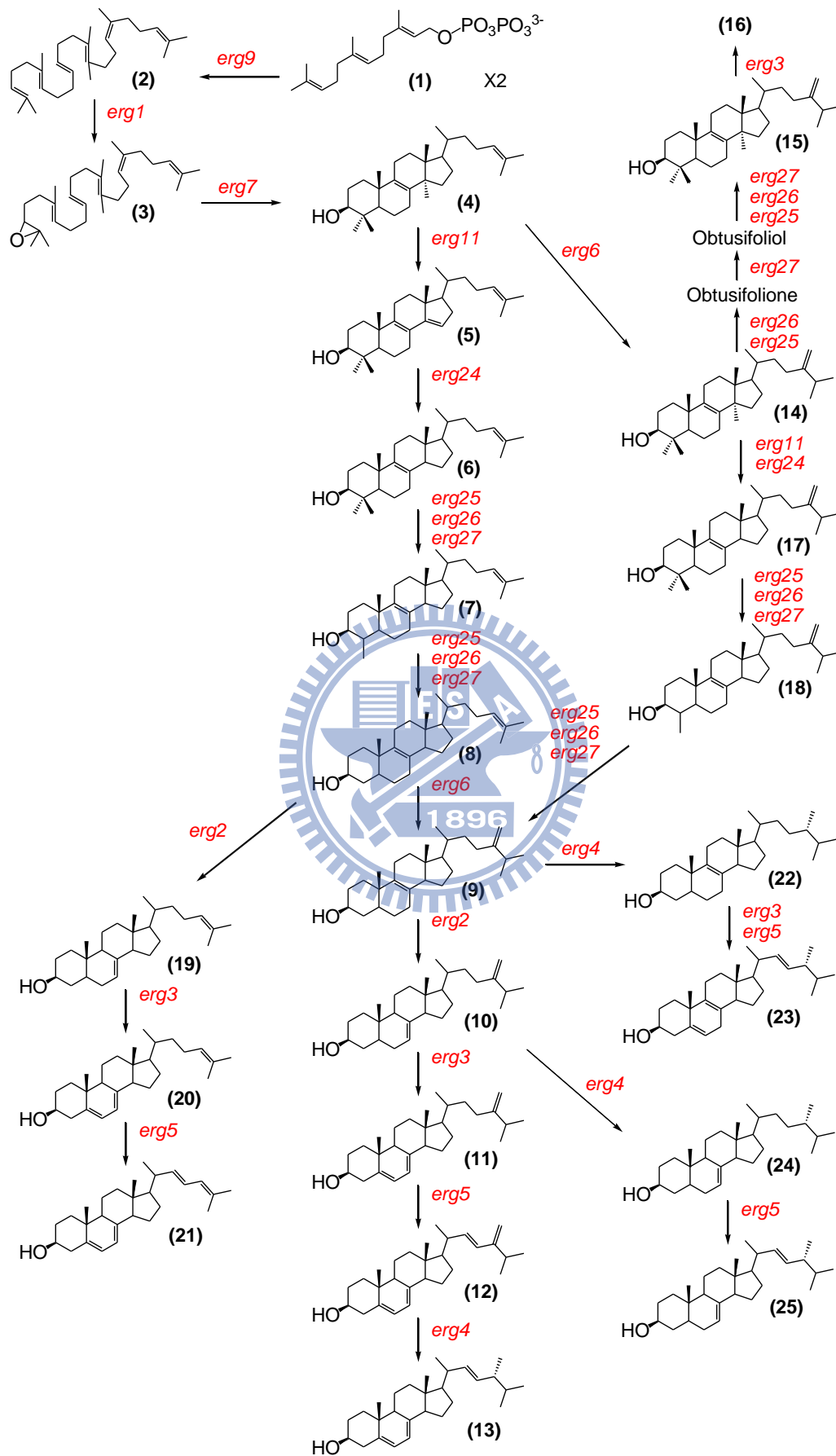
**Figure A.1 Sterol metabolism**

### A.2.3. *erg11* knockout of yeast TKW14C2 strain

The zeocin resistant gene was inserted into *erg11* carried by TOPO vector to block the original function. After *Eco*RI digest, the gel extraction method was used to obtain this gene. Next, the lithium acetate method described in **section A.1.2** was used to substitute the original gene in the yeast strain with the addition of zeocin. Lastly, not only was the genome PCR described in **section A.1.3** used to check the result, but also transformed the normal *erg7* into this knockout strain by electroporation. If the knockout were successful, the strain would die, due to the deficiency of ergosterol.

### A.2.4. Results and Discussion

The check of the zeocin resistant gene by PCR was correct. However, when the *erg7* was transformed into this *erg11* knockout strain, the strain still grew on an ergosterol-deficient plate. There are some possible problems that need to be solved:

i.   The design of *erg11Δ::zeocin$^R$* gene might have some problems.

ii.  The conditions of the lithium acetate method needs improvement.

iii. There might be some unknown pathway involve or interfering, because of the low-specificity enzymes.

iv.  In spite of the problems solved by troubleshooting, the toxic compound, 14α-methylergosta-8,24(28)-dien-3β,6α-diol, is still a problem.

### A.2.5. Future work

According to previous study, the enzymes in sterol metabolic pathways have less specificity, and knocking out the upstream genes cannot block the whole reaction. The only way to maintain compounds at their initial conformation is knockout all of these genes. In addition, the knockout direction is better from

downstream to upstream. Similar to the *erg11* knockout strain, the abnormal pathway lets the product, lanosterol, from *erg7*, transformed into a toxic compound, hence, the unpredictable pathway is dangerous to the yeast strain. After these steps, when the all of these genes knockout strains are constructed, the product will be retained and the analysis will be more precise. Furthermore, by using this strain, the functional investigation of these downstream genes will provide greater insights into enzymatic and pathway functions.

# References

(1)   Sautour, M.; Mitaine-Offer, A. C.; Lacaille-Dubois, M. A. *J. Nat. Med.* **2007**, *61*, 91.

(2)   Connolly, J. D.; Hill, R. A. *Nat. Prod. Rep.* **2002**, *19*, 494.

(3)   Wendt, K. U. *Angew. Chem., Int. Ed.* **2005**, *44*, 3966.

(4)   Woodward, R. B.; Bloch, K. *J. Am. Chem. Soc.* **1953**, *75*, 2023.

(5)   Maudgal, R. K.; Tchen, T. T.; Bloch, K. *J. Am. Chem. Soc.* **1958**, *80*, 2589.

(6)   Cornforth, J. W.; Cornforth, R. H.; Donninger, C.; Popjak, G.; Shimizu, Y.; Ichii, S.; Forchielli, E.; Caspi, E. *J. Am. Chem. Soc.* **1965**, *87*, 3224.

(7)   Van Tamelen, E. E.; Willett, J. D.; Clayton, R. B.; Lord, K. E. *J. Am. Chem. Soc.* **1966**, *88*, 4752.

(8)   Corey, E. J.; Russey, W. E. *J. Am. Chem. Soc.* **1966**, *88*, 4751.

(9)   Van Tamelen, E. E.; Willet, J.; Schwartz, M.; Nadeau, R. *J. Am. Chem. Soc.* **1966**, *88*, 5937.

(10)  Barton, D. H.; Jarman, T. R.; Watson, K. C.; Widdowson, D. A.; Boar, R. B.; Damps, K. *J. Chem. Soc., Perkin Trans. 1* **1975**, 1134.

(11)  Ourisson, G.; Rohmer, M.; Poralla, K. *Annu. Rev. Microbiol.* **1987**, *41*, 301.

(12)  Corey, E. J.; Cheng, H. M.; Baker, C. H.; Matsuda, S. P. T.; Li, D.; Song, X. L. *J. Am. Chem. Soc.* **1997**, *119*, 1277.

(13)  Corey, E. J.; Cheng, H. M.; Baker, C. H.; Matsuda, S. P. T.; Li, D.; Song, X. L. *J. Am. Chem. Soc.* **1997**, *119*, 1289.

(14)  Corey, E. J.; Staas, D. D. *J. Am. Chem. Soc.* **1998**, *120*, 3526.

(15)  Johnson, W. S.; Lindell, S. D.; Steele, J. *J. Am. Chem. Soc.* **1987**, *109*, 5852.

(16)  Johnson, W. S.; Telfer, S. J.; Cheng, S.; Schubert, U. *J. Am. Chem. Soc.* **1987**, *109*, 2517.

(17)  Shi, Z.; Buntel, C. J.; Griffin, J. H. *Proc. Natl. Acad. Sci. U. S. A.* **1994**, *91*, 7370.

(18)  Wendt, K. U.; Poralla, K.; Schulz, G. E. *Science* **1997**, *277*, 1811.

(19)  Wendt, K. U.; Lenhart, A.; Schulz, G. E. *J. Mol. Biol.* **1999**, *286*, 175.

(20)  Reinert, D. J.; Balliano, G.; Schulz, G. E. *Chem. Biol.* **2004**, *11*, 121.

(21)  Abe, I. *Nat. Prod. Rep.* **2007**, *24*, 1311.

(22)  Segura, M. J. R.; Jackson, B. E.; Matsuda, S. P. T. *Nat. Prod. Rep.* **2003**, *20*, 304.

(23)  Corey, E. J.; Virgil, S. C.; Cheng, H. M.; Baker, C. H.; Matsuda, S. P. T.; Singh, V.; Sarshar, S. *J. Am. Chem. Soc.* **1995**, *117*, 11819.

(24)  Wendt, K. U.; Schulz, G. E.; Corey, E. J.; Liu, D. R. *Angew. Chem. Int. Ed. Engl.* **2000**, *39*, 2812.

(25)  Hess, B. A. *Org. Lett.* **2003**, *5*, 165.

(26)  Rajamani, R.; Gao, J. *J. Am. Chem. Soc.* **2003**, *125*, 12768.

(27) Eschenmoser, A.; Ruzicka, L.; Jeger, O.; Arigoni, D. *Helv. Chim. Acta* **1955**, *38*, 1890.

(28) Corey, E. J.; Virgil, S. C. *J. Am. Chem. Soc.* **1991**, *113*, 4025.

(29) Corey, E. J.; Virgil, S. C.; Sarshar, S. *J. Am. Chem. Soc.* **1991**, *113*, 8171.

(30) Thoma, R.; Schulz-Gasch, T.; D'Arcy, B.; Benz, J.; Aebi, J.; Dehmlow, H.; Hennig, M.; Stihle, M.; Ruf, A. *Nature* **2004**, *432*, 118.

(31) Ling, W. H.; Jones, P. J. H. *Life Sci.* **1995**, *57*, 195.

(32) Corey, E. J.; Matsuda, S. P. T.; Bartel, B. *Proc. Natl. Acad. Sci. U. S. A.* **1993**, *90*, 11628.

(33) Lodeiro, S.; Segura, M. J.; Stahl, M.; Schulz-Gasch, T.; Matsuda, S. P. *ChemBioChem* **2004**, *5*, 1581.

(34) Hart, E. A.; Hua, L.; Darr, L. B.; Wilson, W. K.; Pang, J. H.; Matsuda, S. P. T. *J. Am. Chem. Soc.* **1999**, *121*, 9887.

(35) Herrera, J. B. R.; Wilson, W. K.; Matsuda, S. P. T. *J. Am. Chem. Soc.* **2000**, *122*, 6765.

(36) Lodeiro, S.; Schulz-Gasch, T.; Matsuda, S. P. T. *J. Am. Chem. Soc.* **2005**, *127*, 14132.

(37) Kushiro, T.; Shibuya, M.; Ebizuka, Y. *J. Am. Chem. Soc.* **1999**, *121*, 1208.

(38) Kushiro, T.; Shibuya, M.; Masuda, K.; Ebizuka, Y. *J. Am. Chem. Soc.* **2000**, *122*, 6816.

(39) Wu, T. K.; Chang, C. H.; Liu, Y. T.; Wang, T. T. *Chem. Rec.* **2008**, *8*, 302.

(40) Wu, T. K.; Huang, C. Y.; Ko, C. Y.; Chang, C. H.; Chen, Y. J.; Liao, H. K. *Arch. Biochem. Biophys.* **2004**, *421*, 42.

(41) Xiong, Q.; Rocco, F.; Wilson, W. K.; Xu, R.; Ceruti, M.; Matsuda, S. P. *J. Org. Chem.* **2005**, *70*, 5362.

(42) Xu, R.; Fazio, G. C.; Matsuda, S. P. T. *Phytochemistry* **2004**, *65*, 261.

(43) 溫皓宇 *國立交通大學生物科技研究所* **中華民國九十六年**, *碩士論文*.

(44) 張亦諄 *國立交通大學生物醫學研究所* **中華民國九十八年**, *碩士論文*.

(45) Wu, T. K.; Liu, Y. T.; Chiu, F. H.; Chang, C. H. *Org. Lett.* **2006**, *8*, 4691.

(46) Wu, T. K.; Wen, H. Y.; Chang, C. H.; Liu, Y. T. *Org. Lett.* **2008**, *10*, 2529.

(47) Wu, T. K.; Wang, T. T.; Chang, C. H.; Liu, Y. T.; Shie, W. S. *Org. Lett.* **2008**, *10*, 4959.

(48) Sikorski, R. S.; Hieter, P. *Genetics* **1989**, *122*, 19.

(49) Christianson, T. W.; Sikorski, R. S.; Dante, M.; Shero, J. H.; Hieter, P. *Gene* **1992**, *110*, 119.

(50) Schiestl, R. H.; Gietz, R. D. *Curr. Genet.* **1989**, *16*, 339.

(51) Yoshida, Y. *Nippon Nogeikagaku Kaishi-J. Jpn. Soc. Biosci. Biotechol. Agrochem.* **1999**, *73*, 1026.

(52) Kanagasabai, R.; Zhou, W. X.; Liu, J. L.; Nguyen, T. T. M.; Veeramachaneni, P.; Nes, W. D. *Lipids* **2004**, *39*, 737.

(53) Heese-Peck, A.; Pichler, H.; Zanolari, B.; Watanabe, R.; Daum, G.; Riezman, H. *Mol. Biol. Cell* **2002**, *13*, 2664.

(54) Lupetti, A.; Danesi, R.; Campa, M.; Del Tacca, M.; Kelly, S. *Trends Mol. Med.* **2002**, *8*, 76.

(55) Ott, R. G.; Athenstaedt, K.; Hrastnik, C.; Leitner, E.; Bergler, H.; Daum, G. *Biochim. Biophys. Acta Mol. Cell Biol. Lipids* **2005**, *1735*, 111.